PGC-1α isoforms coordinate to balance hepatic metabolism and apoptosis in inflammatory environments

Mélissa Léveillé[1,2]*, Aurèle Besse-Patin[1,2]*, Nathalie Jouvet[1], Aysim Gunes[1], Stewart Jeromson[1,3], Naveen P. Khan[1,3], Sarah Sczelecki[1,3], Cindy Baldwin[1], Annie Dumouchel[1], Jorge Correia[5], Paulo Jannig[5], Stephanie K. Petrillo[4], Anthoula Lazaris[4], Jonathan Boulais[1], Peter Metrakos[4], Jorge L. Ruas[5] and Jennifer L. Estall[1,2,3]¶

*denotes equal contribution

[1]Institut de recherches cliniques de Montreal (IRCM), Montreal, Quebec, Canada.

[2]Faculty of Medicine, University of Montreal, Montreal, Quebec, Canada.

[3]Division of Experimental Medicine, McGill University, Montreal, Quebec, Canada.

[4]Cancer Research Program, Department of Surgery, McGill University Health Center-Research Institute, Montreal, Quebec, H4A 3J1, Canada.

[5]Department of Physiology and Pharmacology, Karolinska Institutet, Stockholm, Sweden.

¶Corresponding author: Jennifer L. Estall, IRCM, 110 avenue des Pins Ouest, Montreal, Quebec, H2W 1R7 Canada. Phone: 514 987 5688, Email: jennifer.estall@ircm.qc.ca

Short title: PGC1A4 inhibits hepatocyte apoptosis

Word count: 6734

Figures: 6 figures, 5 SI Appendix figures

Declaration of interests: The authors have none to declare.

Author contributions:

ML, ABP, NJ, SJ, JLR and JLE designed concept and experiments. ML, ABP, NJ, SJ, NPK, SS, CB, AD, JC, JB and PJ performed and analyzed experiments. SKP, AL, and PM created the human liver biobank, characterized samples, and contributed to analysis design. ML, ABP, NJ, SJ, JLR and JLE wrote the manuscript. All authors reviewed the manuscript.

Grant Support: Research was supported by grants from the CIHR (PJT-148771) and IDRC (108591-001) to JLE, and the Swedish Research Council and Karolinska Institutet to JLR. ML received a doctoral scholarship and JLE a Chercheur-boursier from the FRQS. SJ and NJ are supported by post-doctoral fellowships from Diabetes Canada and the Montreal Diabetes Research Centre, respectively.

Common Abbreviations:

Peroxisome proliferator activated receptor gamma coactivator-1 alpha (PGC-1α); nuclear factor kappa-light-chain-enhancer of activated B cells (NF-κB); tumor necrosis factor alpha (TNFα); non-alcoholic fatty liver disease (NAFLD); non-alcoholic steatohepatitis (NASH)

Transcript Profiling: GEO accession number GSE132458

ABSTRACT

Background and Aims: Liver is exposed to changing metabolic and inflammatory environments. It must sense and adapt to metabolic need while balancing resources required to protect itself from insult. PGC-1α is a transcriptional coactivator that both coordinates metabolic adaptation to diverse stimuli and protects against inflammation in several tissues. However, it is not known how PGC-1α integrates extracellular signals to balance metabolic and anti-inflammatory outcomes. PGC-1α exists as multiple, alternatively spliced variants expressed from different promoters. **Methods:** Tissue samples from transgenic mice and humans with fatty liver disease were analyzed for expression of PGC-1α isoforms and apoptosis caused by inflammatory damage. Primary mouse hepatocytes were used to identify effectors of PGC-1α activity downstream of TNFα. **Results:** We show in human liver that non-alcoholic fatty liver disease (NAFLD) and steatohepatitis (NASH) preferentially activated the alternative *PPARGC1A* promoter. Gene expression analysis in primary mouse hepatocytes identified shared and isoform-specific roles for PGC-1α variants in response to TNFα. PGC-1α1 primarily impacted gene programs of nutrient and mitochondrial metabolism, while TNFα signaling revealed that PGC-1α4 influenced several pathways related to innate immunity and cell death. Gain- and loss-of-function models showed that PGC-1α4 specifically enhanced expression of anti-apoptotic gene programs and attenuated hepatocyte apoptosis in response to TNFα or LPS. This was in contrast to PGC-1α1, which reduced expression of a wide inflammatory gene network, but did not prevent liver cell death. **Conclusions:** We conclude that PGC-1α variants have distinct, yet complimentary roles in hepatic responses to inflammation and identify PGC-1α4 as an important mitigator of apoptosis.

Keywords: liver, PGC-1 isoforms, inflammation, NAFLD, NASH, apoptosis

INTRODUCTION

The unique anatomical architecture of the liver allows it to perform a broad range of metabolic functions, but at the same time it exerts powerful immunocompetence, surveilling portal blood and acting as a protective barrier [1]. The liver must adapt quickly to various metabolic and inflammatory signals from the digestive tract or systemic circulation, concurrently responding to changing glucose and lipid homeostasis. Importantly, hepatic metabolism can be reprogramed by an inflammatory response [2], allowing a trade-off between energy destined for nutrient metabolism versus tolerance to infection. However, mechanisms helping to balance metabolic demand with inflammatory response are not clear.

The peroxisome proliferator activated receptor gamma coactivator-1 alpha (PGC-1α) regulates many transcriptional programs related to nutrient metabolism, energy homeostasis and mitochondrial respiration [3] by binding to nuclear receptors and other transcription factors to enhance their activity [4]. PGC-1α also activates expression of gene programs within a broader set of biological functions in muscle [5-8] and liver [9-14].

Evidence suggests that PGC-1α is also an essential component of the inflammatory response, but mechanisms for this are unclear. Over-expression in muscle protects mice from disease, exercise, and age-related inflammatory damage [15-18] and preservation of PGC-1α activity blunts lipopolysaccharide (LPS)-induced inflammatory damage to heart and kidney [19, 20]. On the other hand, reduced PGC-1α increases pro-inflammatory cytokine expression and increases inflammation damage to muscle and liver tissue in response to stresses [17, 21, 22]. Over-expression of PGC-1α decreases expression of pro-inflammatory cytokines, while simultaneously inducing expression of secreted anti-inflammatory factors [17, 23]. How PGC-1α regulates inflammatory responses and effects of this within cells is not yet understood.

Although PGC-1α is a coactivator, data suggest that PGC-1α may indirectly represses NF-κB target gene transcription though coactivation of anti-inflammatory transcriptional networks

linked to PPARs [18]. It may also bind to the p65 subunit of nuclear factor kappa-light-chain-enhancer of activated B cells (NF-κB) [24]. Thus, mechanistic understanding of links between inflammatory signaling and PGC-1α activity remain limited. Data support PGC-1α as an important regulator of both mitochondria metabolism and inflammation, yet it is not known how PGC-1α integrates multiple extra-cellular signals to coordinate and balance each cellular response. In this study, we show that differentially spliced variants of the PGC-1α protein have unique functions in regulating hepatocyte responses to concurrently integrate metabolic and inflammatory signals.

MATERIALS AND METHODS:

Mice

Hepatocyte-specific PGC-1α knockout mice (LKO: *Ppargc1a*$^{fl/fl,\ Alb\text{-}cre}$) were generated as previously described [10, 11, 22]. Age-matched, male mice on a C57BL/6J background were used. Tissue-specific PGC-1α4 over-expressing mouse line (^{LSL}PGC-1α4) was generated by inserting PGC-1α4 cDNA downstream of a Lox-stop-Lox cassette at the ROSA26 locus (Supplementary Fig. 1). *Ppargc1a* Alternative Promoter Knock-out (AltPromKO) mice were generated by inserting LoxP sites flanking exon 1b and 1b' of the alternative *Ppargc1a* promoter (Supplementary Fig. 1). Experiments were performed in accordance with IRCM institutional animal care and use committee regulations.

Mouse housing, diets, and lipopolysaccharide treatment

Mice were maintained on *ad libitum* chow (Tekland #2918) at 22°C (12h light/dark cycle). For *in vivo* model of steatohepatitis, mice were fed a methionine-choline deficient (MCD) diet (A02082002B, Research Diets) or matched control diet (A02082003B) starting at 8 weeks of age

for up to 42 days. For LPS treatment, livers of 10-week-old male or female mice were harvested 6 hours after tail-vein injection of LPS (2 mg/kg, Invivogen) or vehicle (PBS).

Primary hepatocyte isolation and treatment

Primary mouse hepatocytes from 12-week-old mice were isolated and cultured as previously described [22]. One day after isolation, hepatocytes were infected with adenovirus (5 MOI) overnight and starved of insulin and dexamethasone for 24 hours prior to treatment with tumor necrosis factor alpha (TNFα) (Fitzgerald) at 2 ng/mL for 2 hours for signaling/gene expression, or 20 ng/mL for 8 hours for apoptosis. Apoptosis was measured by Cell Death Detection ELISA (Roche). For reporter assays, cells were transfected (Lipofectamine) with a construct expressing firefly luciferase downstream of 3x NF-κB response elements. Activity was normalized to total protein following quantification using the Dual Luciferase Reporter Assay System (Promega).

Protein isolation, immunoprecipitation and immunoblotting

Proteins were solubilized in radioimmunoprecipitation assay buffer containing protease and phosphatase inhibitors. Hepatic PGC-1α was immunoprecipitated from liver using anti-PGC-1α (Millipore, ST1202) in 1% Triton/TBS. Elutes and total proteins were resolved by SDS-PAGE, blotted, and probed with antibodies (Supplementary Table 1).

Immunofluorescence

H2.35 cells cultured in DMEM, supplemented with 10% Fetal Bovine Serum (FBS, Wisent), 1% penicillin/streptomycin, 0.2 μM dexamethasone were incubated on poly-L-lysine coated coverslips and transfected with V5-tagged PGC-1α variants for 24 hours (Lipofectamine). Cells were starved overnight of dexamethasone prior to TNFα treatment (50 ng/ml) for 3 hours and

fixation with 4% paraformaldehyde. Triton-permeabilized cells were incubated with anti-V5 antibody overnight, followed by Alexa 488-conjugated secondary antibody to visualize proteins.

Cell fractionation

H2.35 cells transduced with adenovirus expressing control vector, PGC-1α1 or PGC-1α4 were starved overnight of dexamethasone prior to TNFα treatment (50 ng/ml) for 3 hours. Cell pellets were washed in PBS and resuspended in Lysis Buffer (10 mM Hepes (pH 7.5), 10 mM KCl, 3 mM $MgCl_2$, 0.35 M sucrose, 0.1% NP40, 3 mM 2-mercaptoethanol, 0.4 mM PMSF, 1 uM pepstatin A, 1 uM leupeptin and 5 ug/ml aprotinin). After centrifugation, supernatants were kept as cytoplasmic fraction. The pellet (nuclear fraction) was washed twice with lysis buffer, resuspended in Buffer A (3 mM EDTA, 0.2 mM EGTA, 1 mM dithiothreitol, 100 mM NaCl and 0.8% NP40) and sonicated for 10 minutes (cycles of 30 seconds ON and 30 seconds OFF). Equal amount of proteins were resolved by SDS-PAGE.

Microarray and Gene set enrichment analysis

mRNA was isolated from primary mouse hepatocytes infected with adenovirus expressing PGC-1α1, PGC-1α4 or vector control treated with 2 ng/mL TNFα or vehicle (PBS) for 2 hours (n = 3) and gene expression profiles generated using Affymetrix Mouse Genome 430 2.0 Arrays. Raw CEL files were normalized using RMA [PMID: 12925520] and annotated using biomaRt [PMID: 16082012]. Raw data and sample annotation are available on GEO (GSE132458).

Gene Set Enrichment Analysis (GSEA) and Gene Ontology (GO) term enrichment were performed on chip data. See Supplementary Methods for details. Full GSEA results are provided in Supplementary File 1. Full GO processes are provided in Supplementary Files 2 (untreated

samples) and 3 (TNFα–treated samples). Gene lists were evaluated for enrichment of transcription factor signatures and binding sites in the proximal promoters and distant regulatory elements using iRegulon and DiRE (http://dire.dcode.org) with default analysis settings.

RNA isolation, PCR, and quantitative RT-PCR.

RNA was isolated from frozen tissue or cells using TRIzol (Invitrogen). 1 μg of RNA treated with DNase I was reverse-transcribed using the High Capacity Reverse Transcription Kit (Applied Biosystems). cDNA was quantified using SYBR Green PCR master mix (Bioline) and normalized to Hypoxanthine-guanine phosphoribosyltransferase (*Hprt*) mRNA using the ΔΔCt threshold cycle method. Presence or absence of PGC-1α variants was confirmed using isoform-specific primers by conventional PCR and sequencing (Supplementary Tables 2 and 3).

Patients and liver samples

Human liver samples were collected from 38 subjects age 33-81 years (Low 3 M: 4 W, NAFLD 10 M: 4 W, NASH 6 M: 3 W, Cirrhotic 4 M: 4 W) undergoing hepatic resection at the McGill University Health Centre after informed consent obtained. Samples were snap-frozen and stored at -80°C. Specimens were scored by a pathologist and classified based on NAFLD Activity Score (NAS: Low =<2, NAFLD =3-5, NASH =6-9, Cirrhotic =7-9) and fibrosis staging from 1A to 3. Study protocol was approved by the Research Ethics Boards of McGill and the Institut de recherches cliniques de Montréal (IRCM). M= men W= women.

Statistical analysis

Sample sizes were based on previous experience with assays and knowledge of expected variance. Normal distribution and homoscedasticity of data were tested by Shapiro–Wilks and Bartlett tests, respectively. Parametric tests were used if distributions normal and variances equal. One-way or Two-way analysis of variance were followed by Tukey's (one-way) or Dunnett's multiple comparisons (two-way) post-hoc test using GraphPad Prism software. Data are expressed as mean ± SEM unless otherwise indicated.

RESULTS

PGC-1α1 and PGC-1α4 are expressed in inflamed liver

PGC-1α mRNA expression is controlled by different promoters (proximal and alternative) induced in a stimulus- and context-dependent manner [25-31] and multiple splice variants of PGC-1α have been identified [32-36]. Using liver tissue from human subjects with biopsy-confirmed inflammatory liver disease (i.e. NAFLD, NASH or cirrhosis), we investigated whether the *PPARGC1A* gene is regulated in fatty liver disease. Splice variants cannot be fully distinguished by qPCR [37]. Using variant-specific non-quantitative PCR, we detected transcripts for *NT-PGC-1α-a* and *PGC-1α1* of the proximal promoter in livers of all conditions, while *PGC-1α-b* and *PGC-1α4* of the alternative promoter were amplified only from livers in subjects with NAFLD and NASH (Fig. 1A). Using quantitative PCR (qPCR), we found only transcripts from the alternative promoter (containing exons 1b and 1b') were increased compared to livers of subjects with simple steatosis (low) (Fig. 1B). Since PGC-1α-b is believed to play a similar role to canonical PGC-1α1 [38], we focused on PGC-1α4, a truncated PGC-1α protein found in muscle to regulate myocyte hypertrophy, but with no known function in liver [34]. By qPCR, transcripts truncated at exon 6 (including *PGC-1α4*) increased proportionally with the severity of inflammatory liver disease (Fig

1C). We also observed similar increases in PGC-1α proteins in livers of mice subjected to a methionine-choline-deficient (MCD) diet, a murine model of inflammatory steatohepatitis (Fig 1D). Taken together, our data suggest that chronic inflammation differentially regulates PGC-1α variant expression and that the induction of the alternative *PPARGC1A* promoter points toward PGC-1α4 being the predominant isoform in inflammatory liver disease.

PGC-1α1 and PGC-1α4 have distinct roles in the hepatic response to TNFα

Since PGC-1α isoforms can have overlapping and distinct biological activity [37], we sought to determine whether PGC-1α1 and PGC-1α4 influence inflammatory signaling pathways. We first compared the transcriptome of primary mouse hepatocytes by microarray following over-expression of PGC-1α1, PGC-1α4, or vector alone in the absence or presence of the inflammatory cytokine TNFα, an inflammatory cytokine associated with NAFLD/NASH (Supplementary Fig. 2). More than 1000 genes changed by ≥2-fold following PGC-1α1 over-expression compared to vector alone (adj. p-value < 0.01), while only 24 were changed by PGC-1α4 and only 4 genes overlapped between the two lists (Fig 2A, Supplementary File 1). Following TNFα treatment, >4500 genes were changed ≥2-fold in hepatocytes over-expressing PGC-1α1 and >3000 for PGC-1α4, with 36% of the genes shared between isoforms (Fig 2A, Supplementary File 2). Clustering of PGC-1α4-modulated genes and comparison to levels in vector- or PGC-1α1-expressing hepatocytes suggested that the activity of PGC-1α4 relied heavily on the presence of TNFα (Fig 2B). Furthermore, within this inflammatory context, PGC-1α4 had both over-lapping and distinct activity from PGC-1α1. Of the 2051 genes shared by the variants in TNFα-treated cells, the majority (91.5%) were regulated in the same manner (positively or negatively, Supplementary File 2).

To gain a global impression of biological process regulated by the PGC-1α variants in hepatocytes, we performed gene set enrichment analysis (GSEA). Gene sets relating to mitochondrial respiration and substrate metabolism were statistically enriched by both PGC-1α1 and PGC-1α4. PGC-1α1 predominantly regulated mitochondrial respiration, and glucose, amino acid and fatty acid metabolism, regardless of TNFα treatment (Supplementary File 3). This is consistent with known roles of PGC-1α1 on mitochondrial metabolism and supported by qPCR (Supplementary Fig. 3). Although we saw no effect of PGC-1α4 on these PGC-1α1 target genes, PGC-1α1 and PGC-1α4 shared many overlapping gene sets (Supplementary File 3). GSEA for PGC-1α4 in untreated hepatocytes centered on lipid metabolism (fatty acids and triglycerides), sterol metabolism and mitochondrial respiration, but individual gene effects were mild and most did not reach the 2-fold cut-off. However, when TNFα was present, PGC-1α4-enriched pathways included regulation of transcription factor transport to the nucleus, innate immunity, responses to interferon/PAMP, TLR signaling, acute inflammation, and apoptosis. Overall, TNFα signaling revealed isoform-specific responses and highlighted processes related to the innate immune response and cell death unique to PGC-1α4.

To explore differential effects of the isoforms on inflammation, we performed gene ontology (GO) analysis on gene changes occurring only in the presence of TNFα. Top 10 GO pathways unique to each variant, or shared, are shown in Fig 2C. All of the top PGC-1α1-regulated processes focused on energy metabolism and were shared with PGC-1α4. However, 6 of the top pathways for PGC-1α4 were unique to this variant, including 6-carbon metabolism, proteolysis, immune signaling in response to pathogens, and regulation of cell death (Fig 2C). Interestingly, GO terms associated with the 175 shared genes regulated in an opposite manner by the variants (Supplementary File 4) centered mainly on cell death and apoptosis (Fig 2D). These data suggest

that apoptosis is an important effector pathway *differentially* regulated by these two PGC-1α protein variants.

TNFα signaling influences localization of PGC-1α4 within liver cells

TNFα treatment substantially increased the number of PGC-1α4 gene targets, revealing that external signals such as inflammation might be necessary for PGC-1α4 activity. We first tested whether TNFα regulates transcription from the *Ppargc1a promoters* using primary mouse hepatocytes. Unlike glucagon treatment, which acutely induces both promoters, TNFα treatment did not change transcript levels from proximal or alternative promoters over a 24-hour period (Fig 3A-B), prompting us to investigate other mechanisms. Over-expressed PGC-1α4 localized primarily to the cytoplasm of liver cells; therefore, nuclear exclusion might explain why increased PGC-1α4 has little effect on basal gene expression in untreated hepatocytes (Fig 2A). Following addition of TNFα to media, a significant proportion of PGC-1α4 was observed in the perinuclear and nuclear compartments (Fig 3C). Cell fractionation confirmed that PGC-1α4 protein was only detected in the nuclear pellet following TNFα treatment (Fig 3C). In contrast, PGC-1α1 localized exclusively to the nucleus of liver cells regardless of treatment condition (Fig 3D).

Increased PGC-1α4 prevents hepatocyte apoptosis in response to inflammatory signaling

Data so far suggested that different PGC-1α isoforms influence inflammatory and anti-apoptotic signals in liver cells. Using gain- and loss-of-function models, we investigated whether PGC-1α1 or PGC-1α4 impacted cell death downstream of inflammatory signals *in vitro* and *in vivo*. Primary mouse hepatocytes over-expressing PGC-1α1 had increased cleaved caspase 3 (Fig 4A) and nucleosome fragmentation (Fig 4B) in response to TNFα treatment compared to vector, while over-expression of PGC-1α4 almost completely blocked apoptosis. To test this *in vivo* and

avoid potentially confounding effects of inflammatory and immune responses caused by viral vectors, we created a transgenic mouse model permitting tissue-specific over-expression of PGC-1α4 (Fig 4C). Recombination at LoxP sites using Albumin promoter-driven Cre-recombinase drove PGC-1α4 expression only in hepatocytes (PGC-1α4^{HepTg}, Fig 4D,E). A small increase in PGC-1α4 transcripts in the absence of Cre-recombinase (^{LSL}PGC-1α4, Fig 4C) indicated a low level of leaky transgene expression, but an increase of ~50-fold expression was observed in livers of PGC-1α4^{HepTg} mice. Supporting an anti-apoptotic role for hepatic PGC-1α4, there were reduced levels of cleaved caspase 3 in livers of both male and female PGC-1α4^{HepTg} mice following injection of LPS (Fig 4F).

Consistent with gain-of-function studies, mice lacking PGC-1α in liver had increased cleaved caspase 3 levels when exposed to LPS (Fig 5A). However, this knockout model ablates all *Ppargc1a* transcripts, making it impossible to discern roles for any specific isoform. Thus, we created a mouse model where only the alternative promoter of *Ppargc1a* was disrupted in a tissue-specific manner (AltProm$^{FL/FL}$), blunting expression of transcripts containing exon 1b and 1b' (including PGC-1α4), but not PGC-1α1 (Fig 5B). To assess efficiency of the promoter knockout, primary hepatocytes from control and KO mice were treated with glucagon, which significantly induced expression of multiple PGC-1α transcripts (Fig 5C) and proteins (Fig 5D) from both the proximal and alternative promoter in control AltProm$^{FL/FL}$ cells. In contrast, ablation of the alternative promoter by crossing floxed mice with Alb-Cre^{Tg} mice (AlbPromKO) blunted induction of alternative transcripts in response to glucagon, yet increases in proximal transcripts were similar to (or even higher than) control cells (Fig 5C). The 37kD PGC-1α protein induced by glucagon was almost completely ablated by knockout of the alternative promoter, identifying PGC-1α4 as the predominant truncated PGC-1α variant responsive to glucagon in liver cells (Fig 5D). Consistent with PGC-1α4 being involved in prevention of apoptosis, hepatocytes

from AlbPromKO mice had higher basal and TNFα-induced cleaved caspase 3 levels (Fig 5E) and increased fragmented nucleosomes in response to inflammatory signaling (Fig 5F) compared to cells from littermate controls. Taken together, PGC-1α4 appears to have the unique ability to prevent inflammatory-mediated apoptosis in liver cells.

PGC-1α isoforms differentially regulate pathways involved in inflammation and cell survival

In an attempt to identify transcription factors with links to apoptosis and cell death downstream of PGC-1α variants, we probed array data for transcription factor motifs enriched in genes changed by PGC-1α1 or PGC-1α4 alone, oppositely regulated by the two variants, or shared when TNFα was present using iRegulon (Supplementary Table S4) and DiRE (Supplementary Fig. 4). Many motifs not previously associated with PGC-1α were identified including: ETV6 (only PGC-1α1); SP4, the NFY complex, IRF6, GM7148, TGIF2, HSF4, and E2F1DP1 (only PGC-1α4); and IRF4, LK4, NR1H2 (LXRβ), ZBTB33 (KAISO), ZFP143, and PITX2 (shared). Among the 175 genes oppositely regulated by the variants, binding sites for STAT, SPIB, NFATC2, and KLF4 were identified. ST18 (also known as MYT3 or NZF3), was found using the gene list implicated in cell survival (Fig 2D). Narrowing analysis to transcription factors implicated in cell death and inflammation, we evaluated whether over-expression of the PGC-1α variants modulated expression of their target genes. PGC-1α4 had no significant effects on mRNA expression, while PGC-1α1 repressed SP4, NF-Y, and STAT targets (Supplementary Fig. 5A,B,C), and increased IRF4 targets *Tnfrsf17* and *Nip3* (Supplementary Fig. 5D).

Our data illustrated that PGC-1α1 and PGC-1α4 had a variety of effects on expression of multiple mediators of inflammation and apoptosis. However, these could not explain opposing effects on cell death observed for the variants in our *in vitro* models. Searching the microarray for

candidate anti-apoptotic genes downstream of PGC-1α4, we identified *Birc2* (*Ciap1*) and *Tnfaip3* (also known as A20) (Fig. 2A), two anti-apoptotic proteins that prevent cell death downstream of inflammatory signalling. In a separate experiment, we confirmed that their transcript levels were significantly higher in mouse primary hepatocytes over-expressing PGC-1α4 only in the presence of TNFα (Fig 6A). Related *Birc3* (*Ciap2*) was also increased by TNFα/PGC-1α4, while *Birc5* expression did not change. In addition, transcripts for apoptosis inhibitors *Naip* and *Xiap* were significantly increased by PGC-1α4, regardless of TNFα treatment. In contrast, over-expression of PGC-1α1 decreased expression of *Birc3, Birc5*, and *Tnfαip3* (Fig 6A) and had no effect on *Naip* and *Xiap.*

Since these genes are all regulated by NF-κB, we hypothesized that PGC-1α4 might enhance NF-κB activity, contrasting with reported repressive effects of PGC-1α1 on this pro-inflammatory transcription factor. Basal expression of a 3x NF-κB response element reporter was increased when PGC-1α1 was co-expressed in primary hepatocytes (Fig 6B); yet consistent with previous findings [18, 24], induction of the reporter by TNFα was significantly blunted by high PGC-1α1. PGC-1α4 had no effect on basal or TNFα-induced NF-κB reporter activity. Protein levels of p50 were decreased by both PGC-1α1 and PGC-1α4 in the presence of TNFα, and p65 remained unchanged in all conditions. Over-expression of PGC-1α1 modestly decreased IKKβ and IκBα proteins, which could relieve inhibition on NF-κB and possibly explain increased basal activity. PGC-1α4 over-expression had no effect on these proteins (Fig 6C). However, consistent with previous reports, increased PGC-1α1 significantly decreased basal and/or TNFα-induced levels of pro-inflammatory genes *Mcp-1*, *Tnfα*, *Iκbα* and *Ccl5* in primary hepatocytes (Fig 6D), demonstrating a strong inhibitory role on NF-κB target genes. In contrast, PGC-1α4 had little impact on these genes, except to potentiate the *Tnfα* response similar to the pattern seen on the anti-apoptotic targets (Fig 6A).

In summary, PGC-1α1 had generally repressive effects on transcription of genes involved in inflammation and cell death that were mostly independent of TNFα. In contrast, PGC-1α4 differentially enhanced a select program of anti-apoptotic factors in hepatocytes only in the presence of inflammatory signaling.

DISCUSSION

In the current study, we found that various non-canonical PGC-1α protein variants are expressed in human and mouse inflamed liver and differentially regulate hepatic inflammatory signaling. Gene set enrichment analysis revealed that in the presence of the inflammatory cytokine TNFα, PGC-1α4 influences innate immunity and cell death, while PGC-1α1 remains primarily associated with mitochondrial function and metabolic processes. Gene ontology (GO) analysis illustrated that genes implicated in cell death and apoptosis appear to be oppositely regulated by these two variants. In primary liver cells, PGC-1α4 significantly blunted apoptosis in response to TNFα, a function that may be controlled by shuttling of PGC-1α4 between cytoplasm and nucleus. We conclude that alternative forms of PGC-1α are induced in inflammatory environments, giving rise to increased levels of the truncated PGC-1α4 isoform that attenuates apoptosis downstream of inflammatory signaling. These findings give mechanistic insight into how PGC-1α, as a family of proteins, facilitate parallel adaptation to metabolic demand and mitigation of inflammatory damage in cells.

Immune responses to danger signals are metabolically challenging and can lead to a trade-off between maintaining highly energy demanding processes of nutrient metabolism versus adaptation to inflammatory stimuli [2]. Inflammation itself may also inhibit metabolism and impede mitochondrial function. Here, we show that signaling via TNFα or LPS leads to a shift in the PGC-1α gene program downstream of PGC-1α1 and PGC-1α4, ensuring that concurrent

inflammatory signaling does not impede the ability to respond to metabolic need. This mechanism represents an additional layer by which the family of PGC-1α proteins help balance an integrated metabolic response modulated by the inflammatory status of the liver.

It is now well established that PGC-1α is a family of proteins created by alternative splicing of the *PPARGC1A* gene in many tissues including skeletal muscle [34, 35, 37], brown adipose tissue [36, 39], and liver [32]. However, a functional role for many of the alternative isoforms remains unknown. While some PGC-1α variants share overlapping functions with canonical PGC-1α1 [29, 30, 33, 38, 40], PGC-1α4 has distinct effector pathways in muscle and brown adipose tissue [34, 41]. We show here that PGC-1α1 and PGC-1α4 also have differential effects on cell death downstream of inflammatory signals. PGC-1α4 almost completely blocks apoptosis *in vitro* and *in vivo*, while PGC-1α1 decreases expression of a broad program of inflammatory genes, but does not inhibit cell death in response to TNFα. PGC-1α1 can induce apoptosis through PPARγ, TFAM, generation of reactive oxygen species, or Ca^{2+} signaling [42-46] or attenuate cell death through a p38/GSK3B/Nrf-2 axis or activation of p53 [47, 48]. Several splice variants coming from differentially regulated promoters adds a layer of complexity, but also may explain existing and often conflicting previous reports.

An obvious candidate effector in inflammation-mediated apoptosis is NF-κB. Consistent with previous studies [49, 50], we show that PGC-1α1 represses NF-κB activity. However, unlike PGC-1α1, our evidence suggests no impact of PGC-1α4 on this transcription factor. Although PGC-1α4 shares the complete activation domain of PGC-1α1, its alternative exon 1 and significant C-terminal truncation may lead PGC-1α4 to regulate a different set of DNA-binding proteins. Our microarray identifies multiple pathways differentially regulated by the two variants, including those targeted by NF-κB, SP4, NF-Y, STAT and IRF4. However, in our model system, PGC-1α4 did not appear to act as a traditional transcriptional coregulator for many of their gene targets. One

possible explanation could be that PGC-1α4 instead promotes novel splicing events to create alternative gene products, similar to the function of related PGC-1α2 and PGC-1α3 variants [51]. Aberrant alternative splicing can substantially affect cellular function and is associated with disease. For example, alternative splicing of TNFα-regulated genes (such as *Tnfaip3*) produces protein variants with distinct roles in cell death and cell survival [52].

While the exclusive nuclear localization of PGC-1α1 supports its function as a transcriptional coactivator, the ability of PGC-1α4 to shuttle between compartments suggests that it might interact with transcription factors in the cytoplasm and/or regulate their entry into the nucleus, a possibility also supported by our GSEA analysis. Interferon (INF) regulatory factors (IRFs) are well-known transcription factors that shuttle in response to inflammatory stimuli [53] and our data suggest that both PGC-1α1 and PGC-1α4 converge on interferon signaling in liver cells. Canonical PGC-1α has been associated with interferon response in the contexts of HCV infection and thermogenesis [54, 55]. Interestingly, three interferon regulatory factors (IRF1, IRF4, IRF6) were identified in our motif enrichment analysis and numerous studies implicate interferons as critical regulators of apoptosis [56, 57]. Although we focused on TNF signaling, our data suggest that PGC-1α1 and PGC-1α4 might also regulate the interferon response; however, further studies are necessary to confirm this hypothesis.

PGC-1α4 shares many similarities to another isoform, NT-PGC-1α, which is transcribed from the proximal promoter. Both have two N-terminal nuclear exclusion signals and three putative phosphorylation (S190, S237, and T252) sites, which regulate nuclear shuttling of NT-PGC-1α [39]. Our data are consistent with reports describing cytoplasmic to nuclear movement of other truncated variants of PGC-1α [36, 39]. Given similarities between these two proteins, it is possible that NT-PGC-1α localization is also regulated by inflammation similar to PGC-1α4, and while likely, it remains to be seen whether PGC-1α4 and NT-PGC-1α have overlapping functions.

We note that only transcripts from the alternative promoter were increased in human NASH and cirrhotic livers. This would suggest that inflammatory signals shift preference from the proximal to the alternative PGC-1α promoter and imply that PGC-1α4 (from the alternative promoter) could be the predominant truncated isoform influencing apoptosis in inflamed human liver. This shift in *PPARGC1A* promoter usage is consistent with previous studies showing a shift to the proximal promoter upon cold exposure in brown adipose tissue and to the alternative promoter upon exercise in skeletal muscle [25-31, 58]. Our data also imply boosting expression of multiple PGC-1α isoforms could allow liver cells to more efficiently respond to energy demand when faced with both high metabolic and inflammatory challenges associated with metabolic disease.

Mechanisms underlying the anti-apoptotic role of hepatic PGC-1α4 appear complex, possibly involving interaction with cytoplasmic proteins, dominant-negative effects on other PGC-1α variants, or regulation of alternative splicing of genes implicated in apoptosis. In conclusion, coordinated activity of these PGC-1α isoforms allows fine-tuning of metabolic and inflammatory networks, supporting efficient adaptation to energy demand within the highly dynamic and inflammatory environment of the liver. Offsetting this balance could result in inefficient nutrient metabolism and/or inappropriate responses to inflammatory stimuli, which may play a role in the pathogenesis of NAFLD or NASH.

ACKNOWLEDGEMENTS

We thank Dr Bruce Spiegelman for generating the AlbProm$^{FL/FL}$ mouse line and members of the IRCM animal, microscopy, and molecular biology core facilities for invaluable technical assistance.

FIGURE LEGENDS

Figure 1: Differential PGC-1α isoform expression in inflamed liver. A,B,C) Expression of known *PPARGC1A* transcripts in human livers. NAS values: LOW ≤ 2 (n=6), NAFLD = 3-5 (n=14), NASH = 6-9 (n=9), CIRRHOSIS = 7-9 + fibrosis (n = 8). A) PCR products specific to each known *PGC-1* α isoform, amplified from cDNA. Lane 9: Water control. B) Quantification of mRNA transcripts containing either exon 1a of the proximal promoter, or exon 1b or exon 1b' of the alternative promoter. Bars represent max. to min., center line represents mean values. Points represent individual human subjects. *p<0.05 compared to low steatosis (LOW). C) mRNA levels of truncated *PGC-1α* isoforms containing alternatively spliced exon 6. D) Western blot of immunoprecipitated PGC-1α proteins (n = 3) from mice given an MCD or control diet.

Figure 2: PGC-1α isoforms differentially regulate inflammatory and metabolic signaling pathways downstream of TNFα.

Gene expression microarrays of mRNA isolated from primary mouse hepatocytes over-expressing either PGC-1α1, PGC-1α4, or vector control by adenoviral infection. A) Number of genes changed greater than 2-fold 48 hr following transduction in the absence or presence of 2 ng/mL TNFα (2 hr) (n = 3 biological replicates, adj. p-value <0.01). B) Clustering of genes significantly changed by over-expression of PGC-1α4 in primary hepatocytes in the presence of TNFα. C) Top 10 GO biological processes (adj. p-value <0.05) were identified from each list generated from TNFα-treated samples in A and listed on x-axis. Size of dot represents number of genes identified in each pathway, in comparison to other genotypes. D) GO biological processes (adj. p-value <0.05) associated with 175 genes regulated in the opposite direction. Data sets were generated using biological replicates (n=3) of each condition from one experiment.

Figure 3: TNFα signaling promotes mobilization of cytoplasmic PGC-1α4 to nuclear and perinuclear regions. A,B) mRNA levels of transcripts expressing either exon 1a of the proximal promoter, or exon 1b of the alternative promoter from primary mouse hepatocytes treated with control (PBS), glucagon (50 nM) or TNFα (20 ng/mL). *p<0.05 TNF effect compared to control, #p<0.05 TNF effect compared to glucagon. C) Confocal imaging of H2.35 mouse liver cells transfected with plasmids expressing V5-tagged PGC-1α1 or PGC-1α4 treated with 50 ng/mL TNFα or vehicle (PBS) for 3 hours. D) Cell fractionation of H2.35 mouse liver cells transduced with adenovirus expressing control vector, PGC-1α1 or PGC-1α4. *non-specific bands. Data are representative of 3 independent experiments.

Figure 4: Over-expression of PGC-1α4 attenuates liver cell apoptosis induced by inflammatory signals. A) Western blot (n=2) and B) fragmented nucleosomes (n=4) in primary mouse hepatocytes over-expressing either PGC-1α1, PGC-1α4, or vector control by adenoviral infection, treated with or without 20 ng/mL TNFα for 8 hours. ***p<0.001 versus vehicle. Data are representative of 3 independent experiments. C) Targeting construct for transgenic mouse allowing tissue-specific over-expression of PGC-1α4 D) mRNA and E) protein from livers of transgenic mice (n = 3) following cross with Albumin-Cre Tg mice to drive PGC-1α4 only in hepatocytes. *p<0.05 versus WT control, n=3 mice. F) Western blot of liver protein from male and female mice 6 hours following tail-vein injection of 2 mg/kg LPS (n = 6 of each sex) or vehicule (PBS) (n = 2 of each sex).

Figure 5: Loss of PGC-1α4 expression enhances apoptosis in response to TNFα. A) Western blot of liver protein from male WT or LKO mice (n = 3 mice) 6 hours following injection of LPS (2 mg/kg) or vehicle (PBS). *p<0.05 versus WT control levels. # p<0.05 versus WT + LPS levels. B)

Targeting construct for creation of mouse allowing tissue-specific ablation of the alternative *Ppargc1a* promoter (AltProm$^{FL/FL}$). C) mRNA of proximal and alternative *Pgc-1*α transcripts and D) western blot of proteins from primary mouse hepatocytes treated with 50 nM glucagon or vehicle. *p<0.05 versus AltProm$^{FL/FL}$ Vehicle. #p<0.05 versus AltPromKO Vehicle, n = 3. E) Western blot and F) fragmented nucleosomes from primary mouse hepatocytes treated with 20 ng/mL TNFα or vehicle for 6 hours. ***p<0.001 versus AltProm$^{FL/FL}$ Vehicle, n = 3. Bars are mean ± SEM of biological replicates in one experiment. Data are representative of 2 independent experiments.

Figure 6: PGC-1α4 potentiates anti-apoptotic gene expression independently of NF-κβ transcriptional coactivation. A) mRNA expression of primary mouse hepatocytes over-expressing PGC-1α1, PGC-1α4 or vector alone following 2-hr treatment with 2 ng/mL TNFα or vehicle (n=3). B) Luciferase activity in primary mouse hepatocytes treated with 2 ng/ml TNFα or vehicle 48 hours following transfection with a 3x NF-κB reporter and constructs for PGC-1α1 or PGC-1α4 (or vector alone, n=3). *p<0.05 genotype effect compared to reporter vector, &p<0.05 TNFα response compared to vehicle, #p<0.05 TNFα response compared to vector + TNFα. C) Western blot and D) mRNA expression of primary mouse hepatocytes over-expressing PGC-1α1, PGC-1α4 or vector following 2-hr treatment with 2 ng/mL TNFα or vehicle (n=3). *p<0.05 effect of TNFα within each genotype. #p<0.05 TNFα response compared to Control + TNFα. $p<0.05 TNFα response compared to PGC-1α1 + TNFα. Data are biological replicates representative of 2-3 independent experiments.

REFERENCES

1. Bogdanos DP, Gao B, Gershwin ME. Liver immunology. Compr Physiol 2013;3:567-98.
2. Ganeshan K, Nikkanen J, Man K, et al. Energetic Trade-Offs and Hypometabolic States Promote Disease Tolerance. Cell 2019;177:399-413 e12.
3. Wu Z, Puigserver P, Andersson U, et al. Mechanisms controlling mitochondrial biogenesis and respiration through the thermogenic coactivator PGC-1. Cell 1999;98:115-24.
4. Kelly DP, Scarpulla RC. Transcriptional regulatory circuits controlling mitochondrial biogenesis and function. Genes Dev 2004;18:357-68.
5. Baar K, Wende AR, Jones TE, et al. Adaptations of skeletal muscle to exercise: rapid increase in the transcriptional coactivator PGC-1. FASEB J 2002;16:1879-86.
6. Handschin C, Kobayashi YM, Chin S, et al. PGC-1alpha regulates the neuromuscular junction program and ameliorates Duchenne muscular dystrophy. Genes Dev 2007;21:770-83.
7. Lin J, Wu H, Tarr PT, et al. Transcriptional co-activator PGC-1 alpha drives the formation of slow-twitch muscle fibres. Nature 2002;418:797-801.
8. Arany Z, Foo SY, Ma Y, et al. HIF-independent regulation of VEGF and angiogenesis by the transcriptional coactivator PGC-1alpha. Nature 2008;451:1008-12.
9. Yoon JC, Puigserver P, Chen G, et al. Control of hepatic gluconeogenesis through the transcriptional coactivator PGC-1. Nature 2001;413:131-8.
10. Estall JL, Kahn M, Cooper MP, et al. Sensitivity of lipid metabolism and insulin signaling to genetic alterations in hepatic peroxisome proliferator-activated receptor-gamma coactivator-1alpha expression. Diabetes 2009;58:1499-508.
11. Estall JL, Ruas JL, Choi CS, et al. PGC-1alpha negatively regulates hepatic FGF21 expression by modulating the heme/Rev-Erb(alpha) axis. Proc Natl Acad Sci U S A 2009;106:22510-5.
12. Besse-Patin A, Jeromson S, Levesque-Damphousse P, et al. PGC1A regulates the IRS1:IRS2 ratio during fasting to influence hepatic metabolism downstream of insulin. Proc Natl Acad Sci U S A 2019.
13. Leone TC, Lehman JJ, Finck BN, et al. PGC-1alpha deficiency causes multi-system energy metabolic derangements: muscle dysfunction, abnormal weight control and hepatic steatosis. PLoS Biol 2005;3:e101.
14. Chambers KT, Chen Z, Lai L, et al. PGC-1beta and ChREBP partner to cooperatively regulate hepatic lipogenesis in a glucose concentration-dependent manner. Mol Metab 2013;2:194-204.
15. Chan MC, Rowe GC, Raghuram S, et al. Post-natal induction of PGC-1alpha protects against severe muscle dystrophy independently of utrophin. Skelet Muscle 2014;4:2.
16. Dinulovic I, Furrer R, Di Fulvio S, et al. PGC-1alpha modulates necrosis, inflammatory response, and fibrotic tissue formation in injured skeletal muscle. Skelet Muscle 2016;6:38.
17. Eisele PS, Furrer R, Beer M, et al. The PGC-1 coactivators promote an anti-inflammatory environment in skeletal muscle in vivo. Biochem Biophys Res Commun 2015;464:692-7.
18. Eisele PS, Salatino S, Sobek J, et al. The peroxisome proliferator-activated receptor gamma coactivator 1alpha/beta (PGC-1) coactivators repress the transcriptional activity of NF-kappaB in skeletal muscle cells. J Biol Chem 2013;288:2246-60.
19. Schilling J, Lai L, Sambandam N, et al. Toll-like receptor-mediated inflammatory signaling reprograms cardiac energy metabolism by repressing peroxisome proliferator-activated receptor gamma coactivator-1 signaling. Circ Heart Fail 2011;4:474-82.

20. Tran M, Tam D, Bardia A, et al. PGC-1alpha promotes recovery after acute kidney injury during systemic inflammation in mice. J Clin Invest 2011;121:4003-14.
21. Sczelecki S, Besse-Patin A, Abboud A, et al. Loss of Pgc-1alpha expression in aging mouse muscle potentiates glucose intolerance and systemic inflammation. Am J Physiol Endocrinol Metab 2014;306:E157-67.
22. Besse-Patin A, Leveille M, Oropeza D, et al. Estrogen Signals Through Peroxisome Proliferator-Activated Receptor-gamma Coactivator 1alpha to Reduce Oxidative Damage Associated With Diet-Induced Fatty Liver Disease. Gastroenterology 2017;152:243-256.
23. Buler M, Aatsinki SM, Skoumal R, et al. Energy-sensing factors coactivator peroxisome proliferator-activated receptor gamma coactivator 1-alpha (PGC-1alpha) and AMP-activated protein kinase control expression of inflammatory mediators in liver: induction of interleukin 1 receptor antagonist. J Biol Chem 2012;287:1847-60.
24. Alvarez-Guardia D, Palomer X, Coll T, et al. The p65 subunit of NF-kappaB binds to PGC-1alpha, linking inflammation and metabolic disturbances in cardiac cells. Cardiovasc Res 2010;87:449-58.
25. Chinsomboon J, Ruas J, Gupta RK, et al. The transcriptional coactivator PGC-1alpha mediates exercise-induced angiogenesis in skeletal muscle. Proc Natl Acad Sci U S A 2009;106:21401-6.
26. Norrbom J, Sallstedt EK, Fischer H, et al. Alternative splice variant PGC-1alpha-b is strongly induced by exercise in human skeletal muscle. Am J Physiol Endocrinol Metab 2011;301:E1092-8.
27. Popov DV, Bachinin AV, Lysenko EA, et al. Exercise-induced expression of peroxisome proliferator-activated receptor gamma coactivator-1alpha isoforms in skeletal muscle of endurance-trained males. J Physiol Sci 2014;64:317-23.
28. Tadaishi M, Miura S, Kai Y, et al. Effect of exercise intensity and AICAR on isoform-specific expressions of murine skeletal muscle PGC-1alpha mRNA: a role of beta(2)-adrenergic receptor activation. Am J Physiol Endocrinol Metab 2011;300:E341-9.
29. Thom R, Rowe GC, Jang C, et al. Hypoxic induction of vascular endothelial growth factor (VEGF) and angiogenesis in muscle by truncated peroxisome proliferator-activated receptor gamma coactivator (PGC)-1alpha. J Biol Chem 2014;289:8810-7.
30. Wen X, Wu J, Chang JS, et al. Effect of exercise intensity on isoform-specific expressions of NT-PGC-1 alpha mRNA in mouse skeletal muscle. Biomed Res Int 2014;2014:402175.
31. Ydfors M, Fischer H, Mascher H, et al. The truncated splice variants, NT-PGC-1alpha and PGC-1alpha4, increase with both endurance and resistance exercise in human skeletal muscle. Physiol Rep 2013;1:e00140.
32. Felder TK, Soyal SM, Oberkofler H, et al. Characterization of novel peroxisome proliferator-activated receptor gamma coactivator-1alpha (PGC-1alpha) isoform in human liver. J Biol Chem 2011;286:42923-36.
33. Miura S, Kai Y, Kamei Y, et al. Isoform-specific increases in murine skeletal muscle peroxisome proliferator-activated receptor-gamma coactivator-1alpha (PGC-1alpha) mRNA in response to beta2-adrenergic receptor activation and exercise. Endocrinology 2008;149:4527-33.
34. Ruas JL, White JP, Rao RR, et al. A PGC-1alpha isoform induced by resistance training regulates skeletal muscle hypertrophy. Cell 2012;151:1319-31.
35. Yoshioka T, Inagaki K, Noguchi T, et al. Identification and characterization of an alternative promoter of the human PGC-1alpha gene. Biochem Biophys Res Commun 2009;381:537-43.

36. Zhang Y, Huypens P, Adamson AW, et al. Alternative mRNA splicing produces a novel biologically active short isoform of PGC-1alpha. J Biol Chem 2009;284:32813-26.
37. Martinez-Redondo V, Pettersson AT, Ruas JL. The hitchhiker's guide to PGC-1alpha isoform structure and biological functions. Diabetologia 2015;58:1969-77.
38. Tadaishi M, Miura S, Kai Y, et al. Skeletal muscle-specific expression of PGC-1alpha-b, an exercise-responsive isoform, increases exercise capacity and peak oxygen uptake. PLoS One 2011;6:e28290.
39. Chang JS, Huypens P, Zhang Y, et al. Regulation of NT-PGC-1alpha subcellular localization and function by protein kinase A-dependent modulation of nuclear export by CRM1. J Biol Chem 2010;285:18039-50.
40. Chang JS, Jun HJ, Park M. Transcriptional coactivator NT-PGC-1alpha promotes gluconeogenic gene expression and enhances hepatic gluconeogenesis. Physiol Rep 2016;4.
41. Chang JS, Fernand V, Zhang Y, et al. NT-PGC-1alpha protein is sufficient to link beta3-adrenergic receptor activation to transcriptional and physiological components of adaptive thermogenesis. J Biol Chem 2012;287:9100-11.
42. Bianchi K, Vandecasteele G, Carli C, et al. Regulation of Ca2+ signalling and Ca2+-mediated cell death by the transcriptional coactivator PGC-1alpha. Cell Death Differ 2006;13:586-96.
43. Zhang Y, Ba Y, Liu C, et al. PGC-1alpha induces apoptosis in human epithelial ovarian cancer cells through a PPARgamma-dependent pathway. Cell Res 2007;17:363-73.
44. Onishi Y, Ueha T, Kawamoto T, et al. Regulation of mitochondrial proliferation by PGC-1alpha induces cellular apoptosis in musculoskeletal malignancies. Sci Rep 2014;4:3916.
45. Adhihetty PJ, Uguccioni G, Leick L, et al. The role of PGC-1alpha on mitochondrial function and apoptotic susceptibility in muscle. Am J Physiol Cell Physiol 2009;297:C217-25.
46. D'Errico I, Salvatore L, Murzilli S, et al. Peroxisome proliferator-activated receptor-gamma coactivator 1-alpha (PGC1alpha) is a metabolic regulator of intestinal epithelial cell fate. Proc Natl Acad Sci U S A 2011;108:6603-8.
47. Choi HI, Kim HJ, Park JS, et al. PGC-1alpha attenuates hydrogen peroxide-induced apoptotic cell death by upregulating Nrf-2 via GSK3beta inactivation mediated by activated p38 in HK-2 Cells. Sci Rep 2017;7:4319.
48. Sen N, Satija YK, Das S. PGC-1alpha, a key modulator of p53, promotes cell survival upon metabolic stress. Mol Cell 2011;44:621-34.
49. Eisele PS, Handschin C. Functional crosstalk of PGC-1 coactivators and inflammation in skeletal muscle pathophysiology. Semin Immunopathol 2014;36:27-53.
50. Zhang Y, Chen C, Jiang Y, et al. PPARgamma coactivator-1alpha (PGC-1alpha) protects neuroblastoma cells against amyloid-beta (Abeta) induced cell death and neuroinflammation via NF-kappaB pathway. BMC Neurosci 2017;18:69.
51. Martinez-Redondo V, Jannig PR, Correia JC, et al. Peroxisome Proliferator-activated Receptor gamma Coactivator-1 alpha Isoforms Selectively Regulate Multiple Splicing Events on Target Genes. J Biol Chem 2016;291:15169-84.
52. Lopez-Urrutia E, Campos-Parra A, Herrera LA, et al. Alternative splicing regulation in tumor necrosis factor-mediated inflammation. Oncol Lett 2017;14:5114-5120.
53. Reich NC. Nuclear/cytoplasmic localization of IRFs in response to viral infection or interferon stimulation. J Interferon Cytokine Res 2002;22:103-9.
54. Shlomai A, Rechtman MM, Burdelova EO, et al. The metabolic regulator PGC-1alpha links hepatitis C virus infection to hepatic insulin resistance. J Hepatol 2012;57:867-73.

55. Kong X, Banks A, Liu T, et al. IRF4 is a key thermogenic transcriptional partner of PGC-1alpha. Cell 2014;158:69-83.
56. Chattopadhyay S, Marques JT, Yamashita M, et al. Viral apoptosis is induced by IRF-3-mediated activation of Bax. EMBO J 2010;29:1762-73.
57. Kim PK, Armstrong M, Liu Y, et al. IRF-1 expression induces apoptosis and inhibits tumor growth in mouse mammary cancer cells in vitro and in vivo. Oncogene 2004;23:1125-35.
58. Popov DV, Lysenko EA, Vepkhvadze TF, et al. Promoter-specific regulation of PPARGC1A gene expression in human skeletal muscle. J Mol Endocrinol 2015;55:159-68.

Figure 1

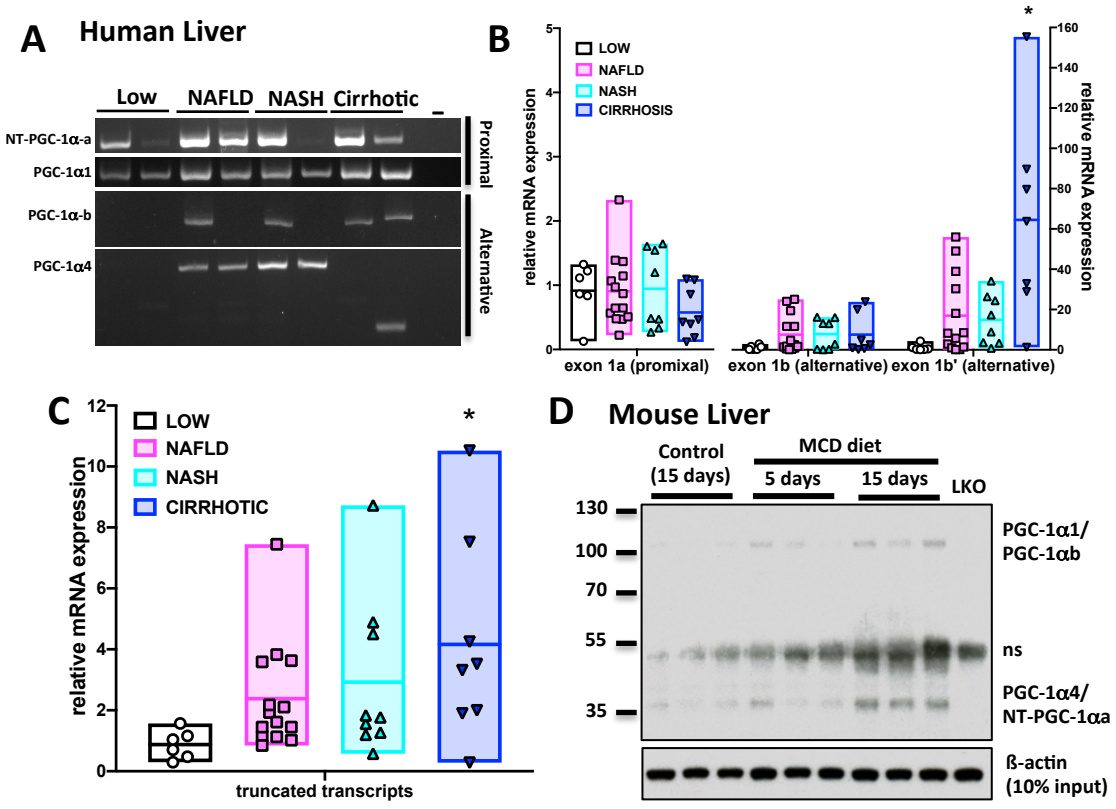
A
Human Liver
Low
NAFLD
NASH
Cirrhotic
NT-PGC-1α-a
PGC-1α1
PGC-1α-b
PGC-1α4
Proximal
Alternative
B
LOW
NAFLD
NASH
CIRRHOSIS
relative mRNA expression
relative mRNA expression
exon 1a (promixal)
exon 1b (alternative)
exon 1b' (alternative)
*
C
LOW
NAFLD
NASH
CIRRHOTIC
relative mRNA expression
truncated transcripts
*
D
Mouse Liver
Control
(15 days)
MCD diet
5 days
15 days
LKO
130
100
70
55
35
PGC-1α1/
PGC-1αb
ns
PGC-1α4/
NT-PGC-1αa
ß-actin
(10% input)

Figure 2

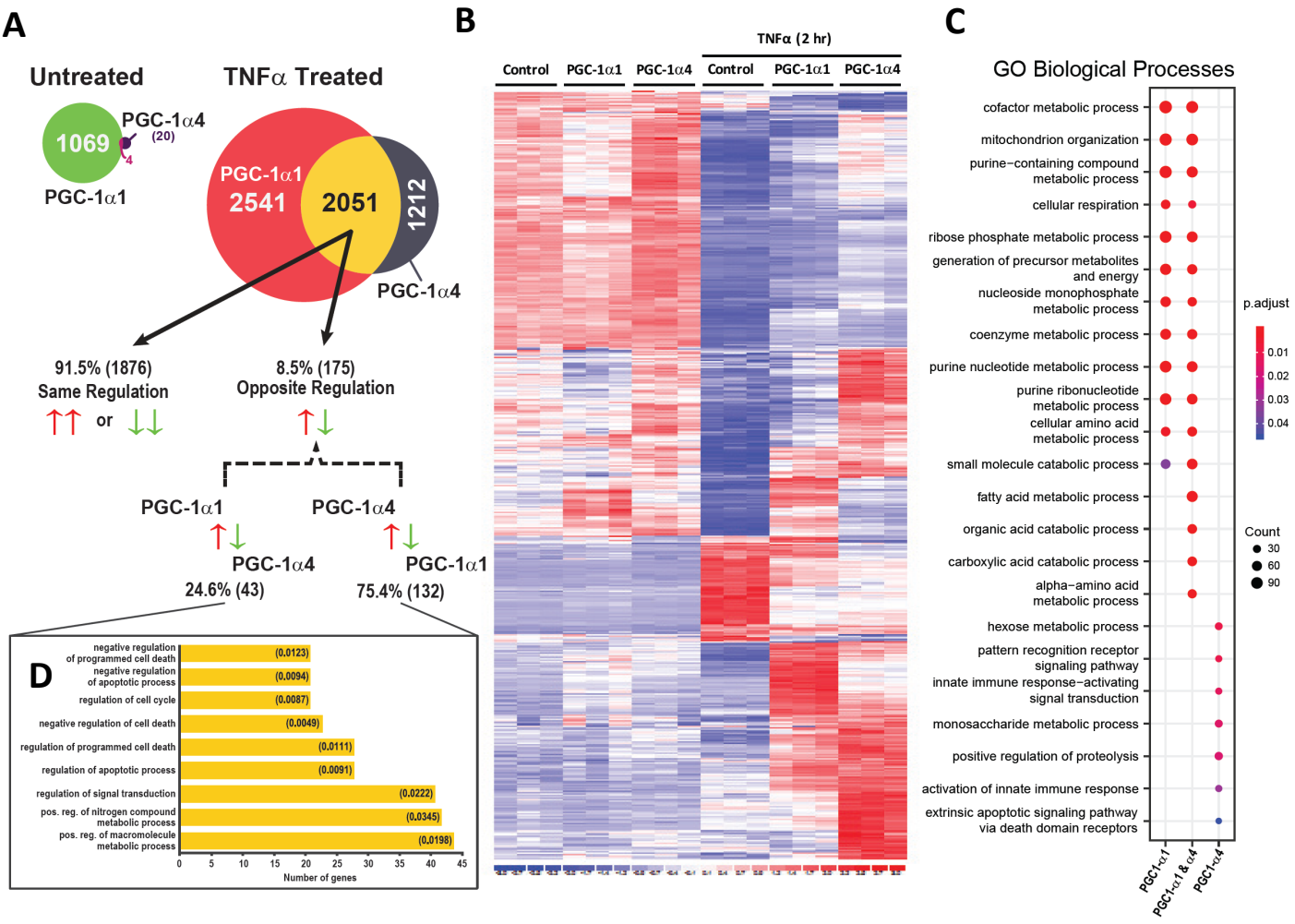
A
Untreated
TNFα Treated
1069
PGC-1α4
(20)
4
PGC-1α1
PGC-1α1
2541
2051
1212
PGC-1α4
91.5% (1876)
Same Regulation
or
8.5% (175)
Opposite Regulation
PGC-1α1
PGC-1α4
PGC-1α4
PGC-1α1
24.6% (43)
75.4% (132)
D
negative regulation of programmed cell death (0.0123)
negative regulation of apoptotic process (0.0094)
regulation of cell cycle (0.0087)
negative regulation of cell death (0.0049)
regulation of programmed cell death (0.0111)
regulation of apoptotic process (0.0091)
regulation of signal transduction (0.0222)
pos. reg. of nitrogen compound metabolic process (0.0345)
pos. reg. of macromolecule metabolic process (0.0198)
0 5 10 15 20 25 30 35 40 45
Number of genes
B
TNFα (2 hr)
Control
PGC-1α1
PGC-1α4
Control
PGC-1α1
PGC-1α4
C
GO Biological Processes
cofactor metabolic process
mitochondrion organization
purine−containing compound metabolic process
cellular respiration
ribose phosphate metabolic process
generation of precursor metabolites and energy
nucleoside monophosphate metabolic process
coenzyme metabolic process
purine nucleotide metabolic process
purine ribonucleotide metabolic process
cellular amino acid metabolic process
small molecule catabolic process
fatty acid metabolic process
organic acid catabolic process
carboxylic acid catabolic process
alpha−amino acid metabolic process
hexose metabolic process
pattern recognition receptor signaling pathway
innate immune response−activating signal transduction
monosaccharide metabolic process
positive regulation of proteolysis
activation of innate immune response
extrinsic apoptotic signaling pathway via death domain receptors
PGC1−α1
PGC1−α1 & α4
PGC1−α4
p.adjust
0.01
0.02
0.03
0.04
Count
30
60
90

Figure 3

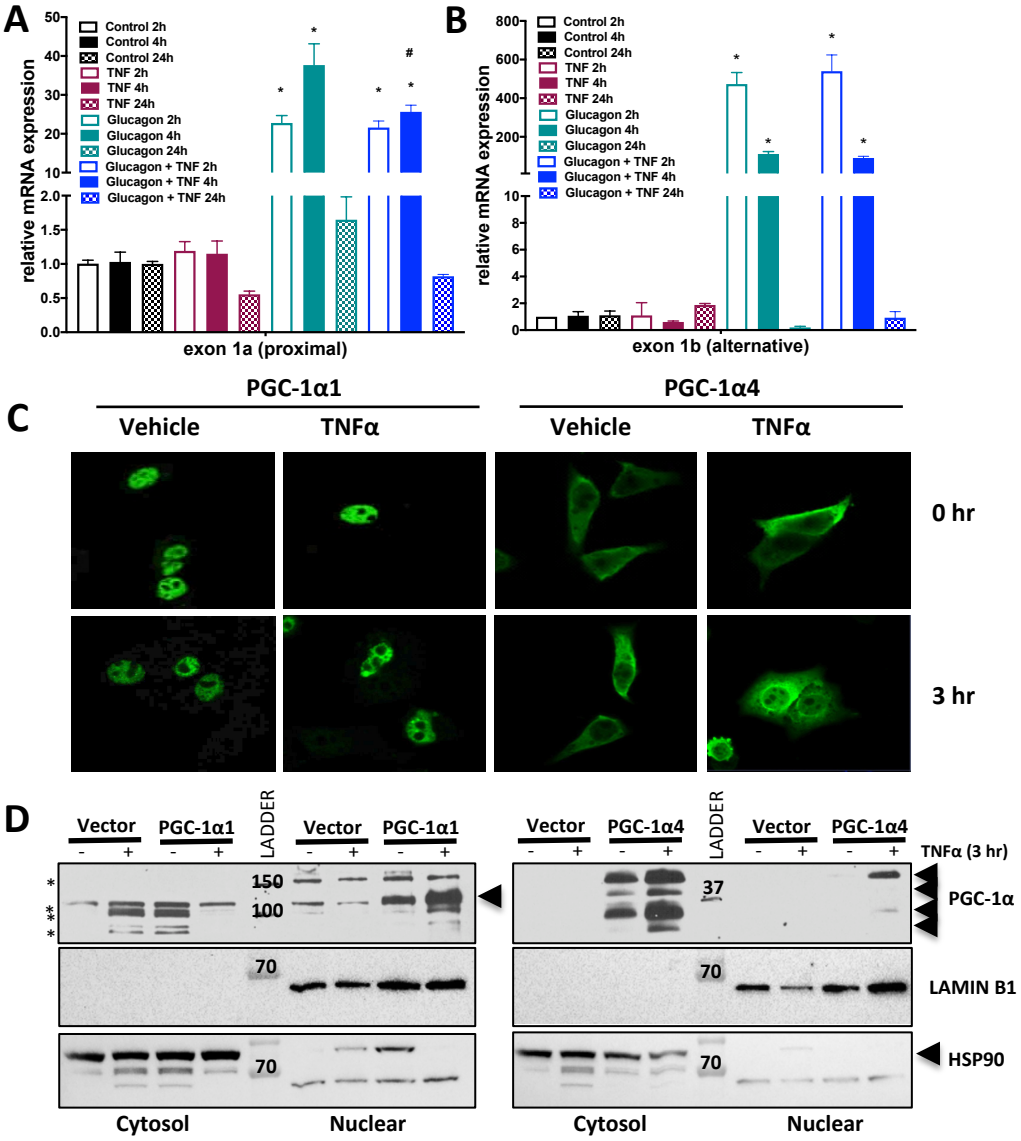
A
B
relative mRNA expression
Control 2h
Control 4h
Control 24h
TNF 2h
TNF 4h
TNF 24h
Glucagon 2h
Glucagon 4h
Glucagon 24h
Glucagon + TNF 2h
Glucagon + TNF 4h
Glucagon + TNF 24h
exon 1a (proximal)
exon 1b (alternative)
C
PGC-1α1
PGC-1α4
Vehicle
TNFα
0 hr
3 hr
D
Vector
PGC-1α1
PGC-1α4
LADDER
TNFα (3 hr)
PGC-1α
LAMIN B1
HSP90
Cytosol
Nuclear

Figure 4

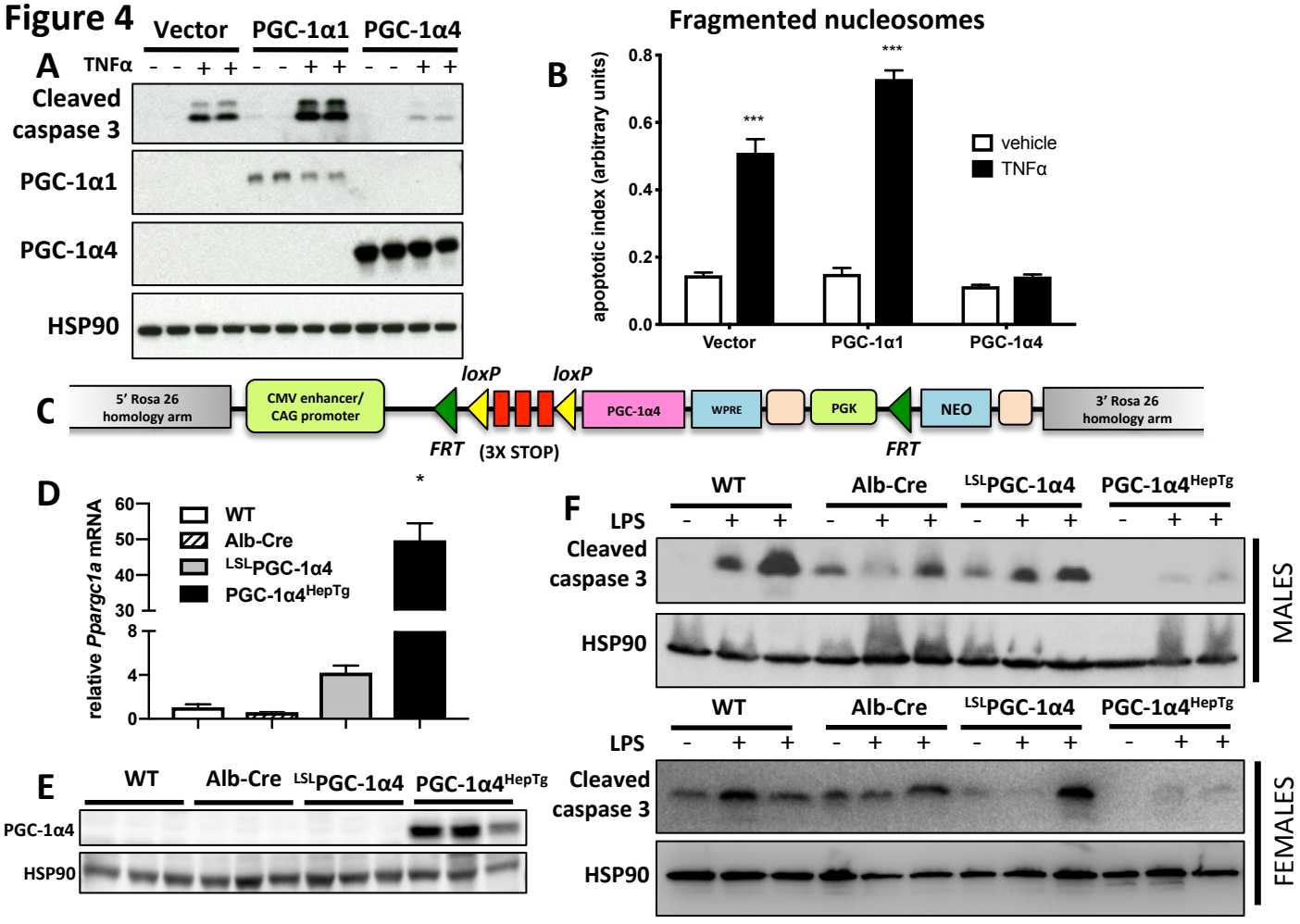
A
Vector
PGC-1α1
PGC-1α4
TNFα
Cleaved caspase 3
PGC-1α1
PGC-1α4
HSP90
B
Fragmented nucleosomes
apoptotic index (arbitrary units)
vehicle
TNFα
Vector
PGC-1α1
PGC-1α4
C
5' Rosa 26 homology arm
CMV enhancer/ CAG promoter
loxP
loxP
FRT
(3X STOP)
PGC-1α4
WPRE
PGK
NEO
FRT
3' Rosa 26 homology arm
D
relative Ppargc1a mRNA
WT
Alb-Cre
LSLPGC-1α4
PGC-1α4HepTg
E
WT
Alb-Cre
LSLPGC-1α4
PGC-1α4HepTg
PGC-1α4
HSP90
F
WT
Alb-Cre
LSLPGC-1α4
PGC-1α4HepTg
LPS
Cleaved caspase 3
HSP90
MALES
FEMALES

Figure 5

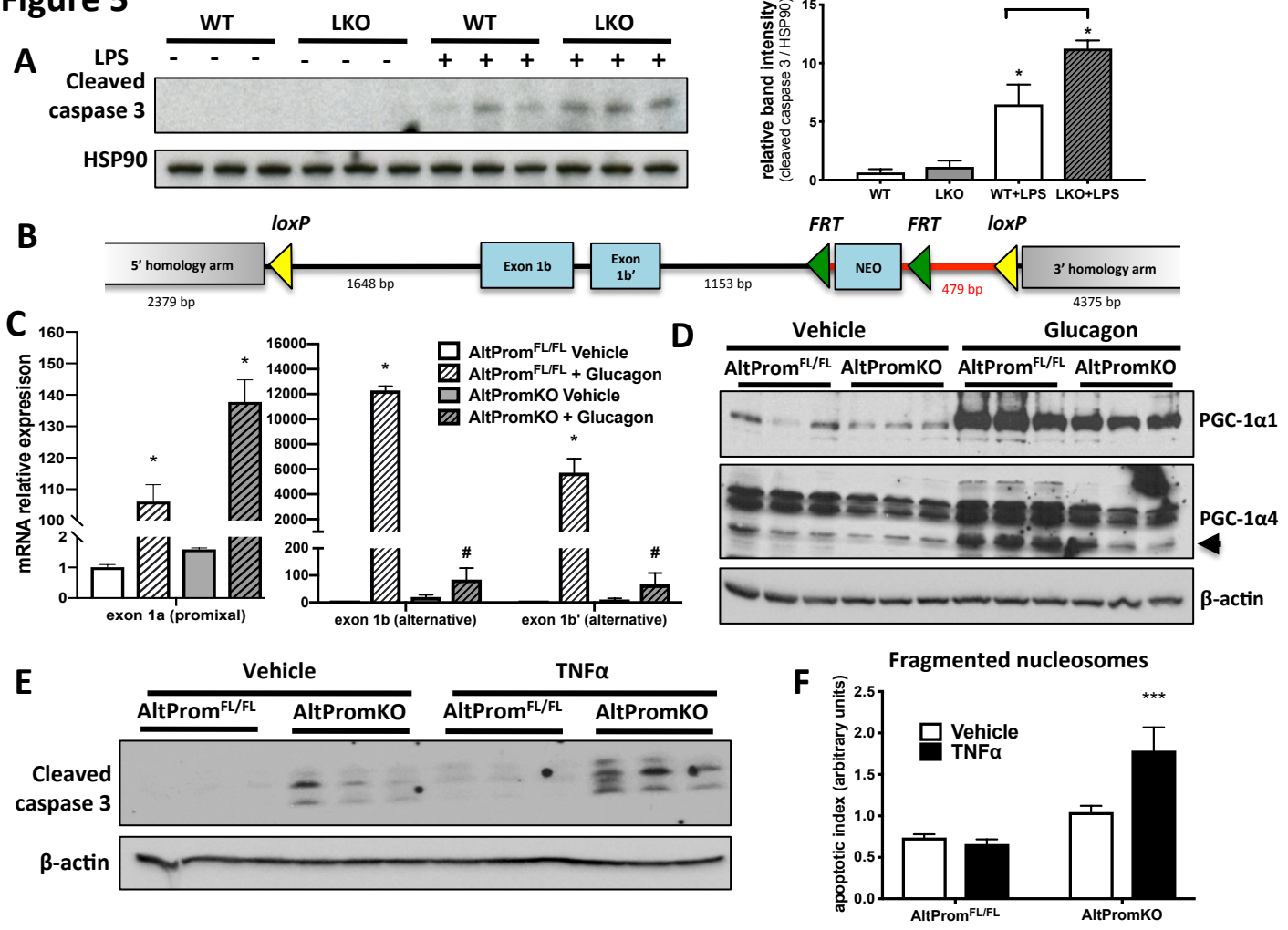
A
WT
LKO
WT
LKO
LPS
Cleaved caspase 3
HSP90
relative band intensity (cleaved caspase 3 / HSP90)
WT
LKO
WT+LPS
LKO+LPS
B
loxP
FRT
FRT
loxP
5' homology arm
Exon 1b
Exon 1b'
NEO
3' homology arm
2379 bp
1648 bp
1153 bp
479 bp
4375 bp
C
mRNA relative expresison
AltProm FL/FL Vehicle
AltProm FL/FL + Glucagon
AltPromKO Vehicle
AltPromKO + Glucagon
exon 1a (promixal)
exon 1b (alternative)
exon 1b' (alternative)
D
Vehicle
Glucagon
AltProm FL/FL
AltPromKO
PGC-1α1
PGC-1α4
β-actin
E
Vehicle
TNFα
AltProm FL/FL
AltPromKO
Cleaved caspase 3
β-actin
F
Fragmented nucleosomes
apoptotic index (arbitrary units)
Vehicle
TNFα
AltProm FL/FL
AltPromKO

Figure 6

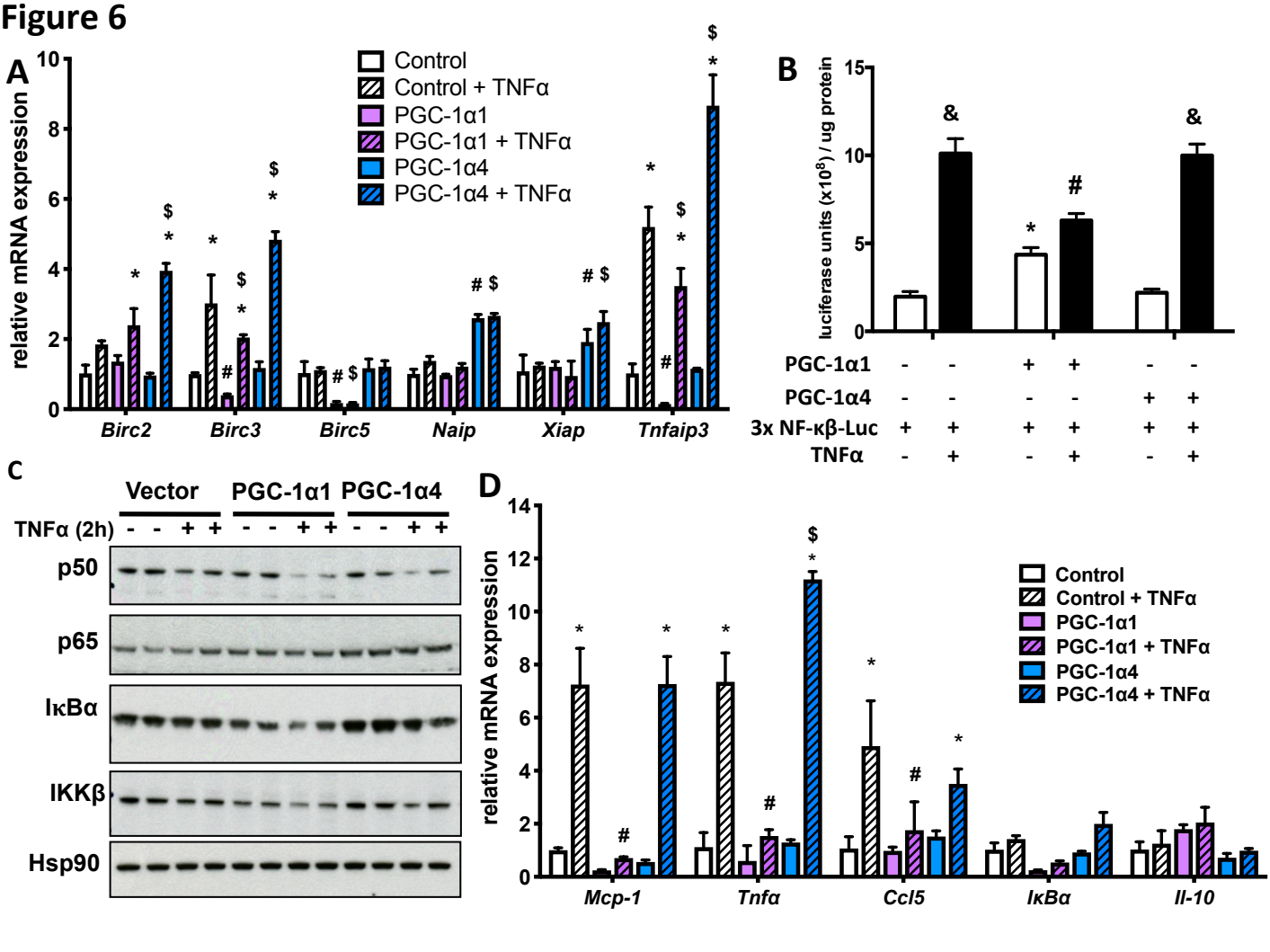
A
relative mRNA expression
Control
Control + TNFα
PGC-1α1
PGC-1α1 + TNFα
PGC-1α4
PGC-1α4 + TNFα
Birc2
Birc3
Birc5
Naip
Xiap
Tnfaip3
B
luciferase units (x10^8) / ug protein
PGC-1α1
PGC-1α4
3x NF-κβ-Luc
TNFα
C
Vector
PGC-1α1
PGC-1α4
TNFα (2h)
p50
p65
IκBα
IKKβ
Hsp90
D
relative mRNA expression
Control
Control + TNFα
PGC-1α1
PGC-1α1 + TNFα
PGC-1α4
PGC-1α4 + TNFα
Mcp-1
Tnfα
Ccl5
IκBα
Il-10

Supplementary Figure 1

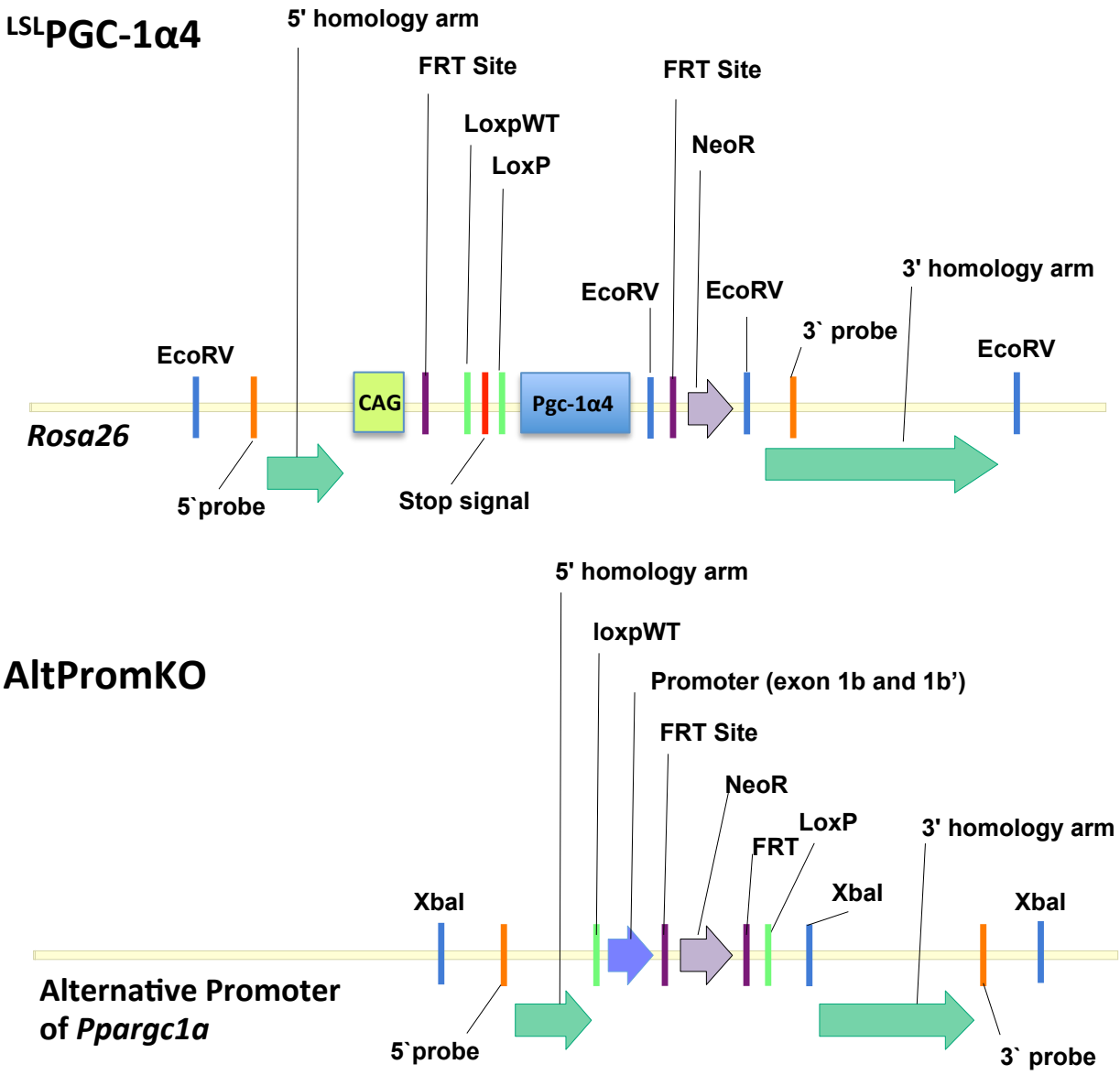

Supplementary Figure 1: Targeting strategies for ^{LSL}PGC-1α4 and AltPromKO mouse lines. Schematic of genomic locus for each mouse line, following recombination. Restriction sites (blue) and DNA probes (orange) used for Southern blot screening of ES clones are indicated. Complete diagrams of regulatory and cDNA elements inserted into genome can be found in Figures 4 and 5. The ^{LSL}PGC-1α4 was generated by replacing tdTomato with murine PGC-1α4 cDNA in the Ai9 vector downstream of the Lox-stop-Lox signal. Recombination at the *ROSA26* locus was confirmed in neomycin-resistant C57BL/6 embryonic stem cells clones and founder mice backcrossed 10 generations onto a C57BL/6N background. The AltPromKO was generated by InGenious Targeting Laboratory (Ronkonkoma, New York). A targeting construct was used to insert LoxP sites flanking exon 1b and 1b' of the alternative *Ppargc1a* promoter. Recombination was confirmed in C57BL/6 embryonic stem cells and founder mice backcrossed three times with C57BL/6N mice.

Supplementary Figure 2

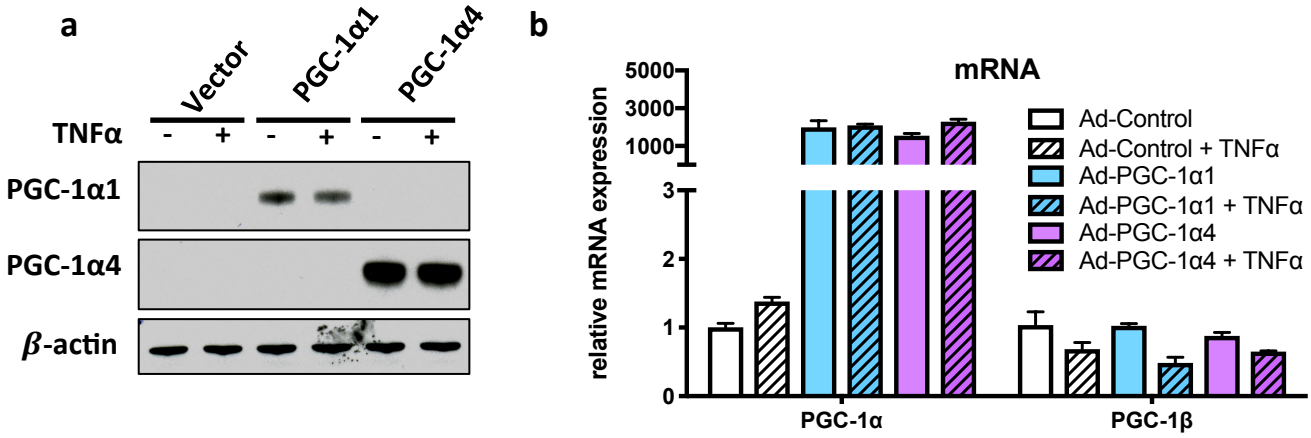

Supplementary Figure 2: Relative levels of PGC-1 mRNA and protein following over-expression in primary mouse hepatocytes and TNFα treatment. a) Western blot of proteins and b) relative mRNA levels in primary hepatocytes 48 hours following transduction with an adenovirus expressing cDNA for PGC-1α1, PGC-1α4 or vector alone (Ad-CMV-GFP). Prior to harvest, cells were treated for 2 hours with 20 ng/mL TNFα or vehicle alone (PBS).

Supplementary Figure 3

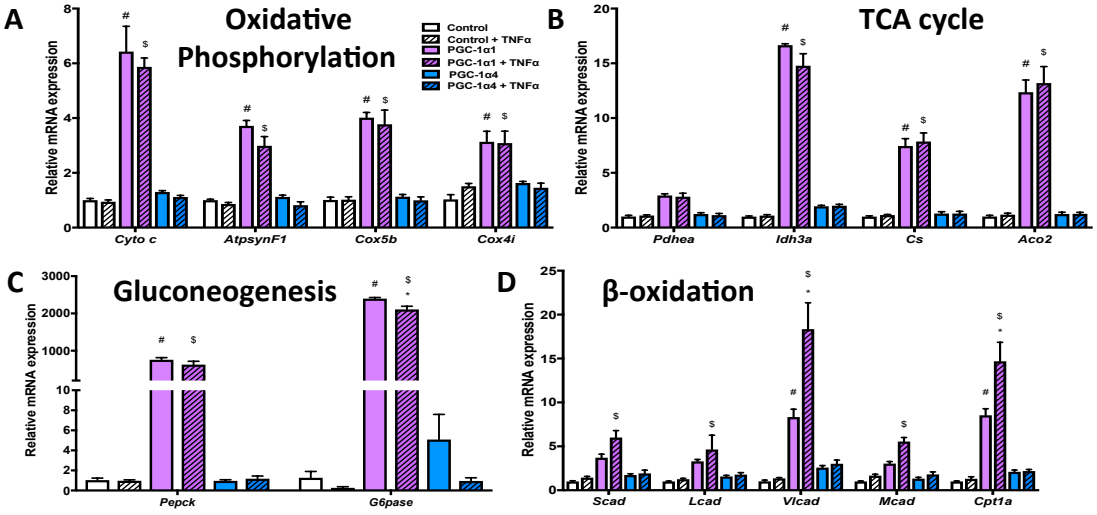

Supplementary Figure 3: PGC-1α isoforms differentially regulate metabolic genes downstream of TNFα. A-D) mRNA expression of primary mouse hepatocytes over-expressing PGC-1α1, PGC-1α4 or vector alone following 2-hr treatment with 2 ng/mL TNFα or vehicle (n=3). *p<0.05 effect of TNFα within each genotype. #p<0.05 Effect of PGC-1α1 or PGC-1α4 expression compared to Control. $p<0.05 TNFα response compared to Control + TNFα. Data is representative biological replicates (n=3) from one experiment performed at least 3 independent times.

Supplementary Figure 4

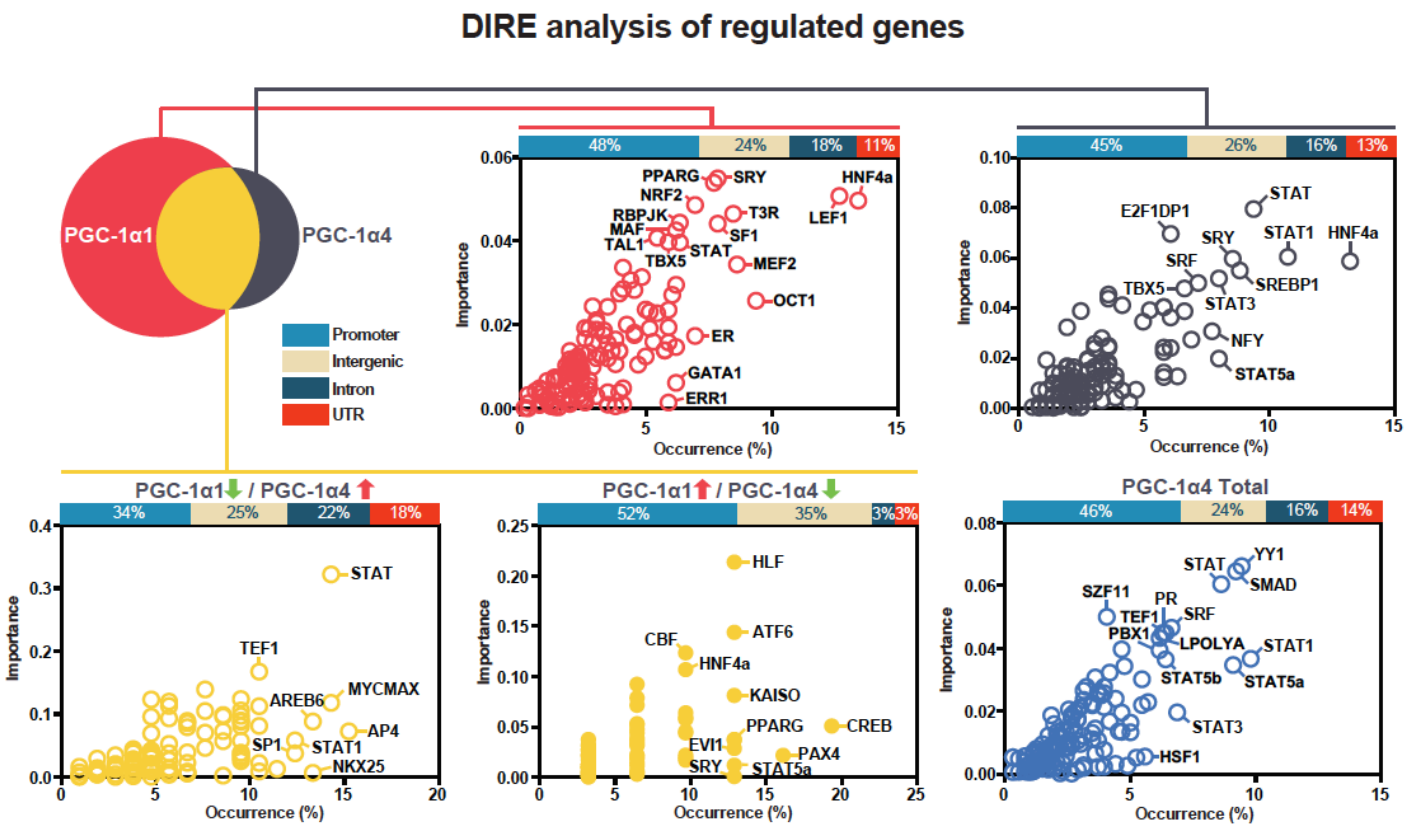

Supplementary Figure 4: DiRE analysis of regulatory regions for enrichment of transcription factor binding sites. Plotted are the occurrence of each binding motif and its importance metric, which reflects binding site specificity to the input gene set, compared to a background random set of 5000 genes. The top horizontal bars depict relative distribution of identified regulatory elements in promoters, intergenic, intronic, or untranslated regions.

Supplementary Figure 5

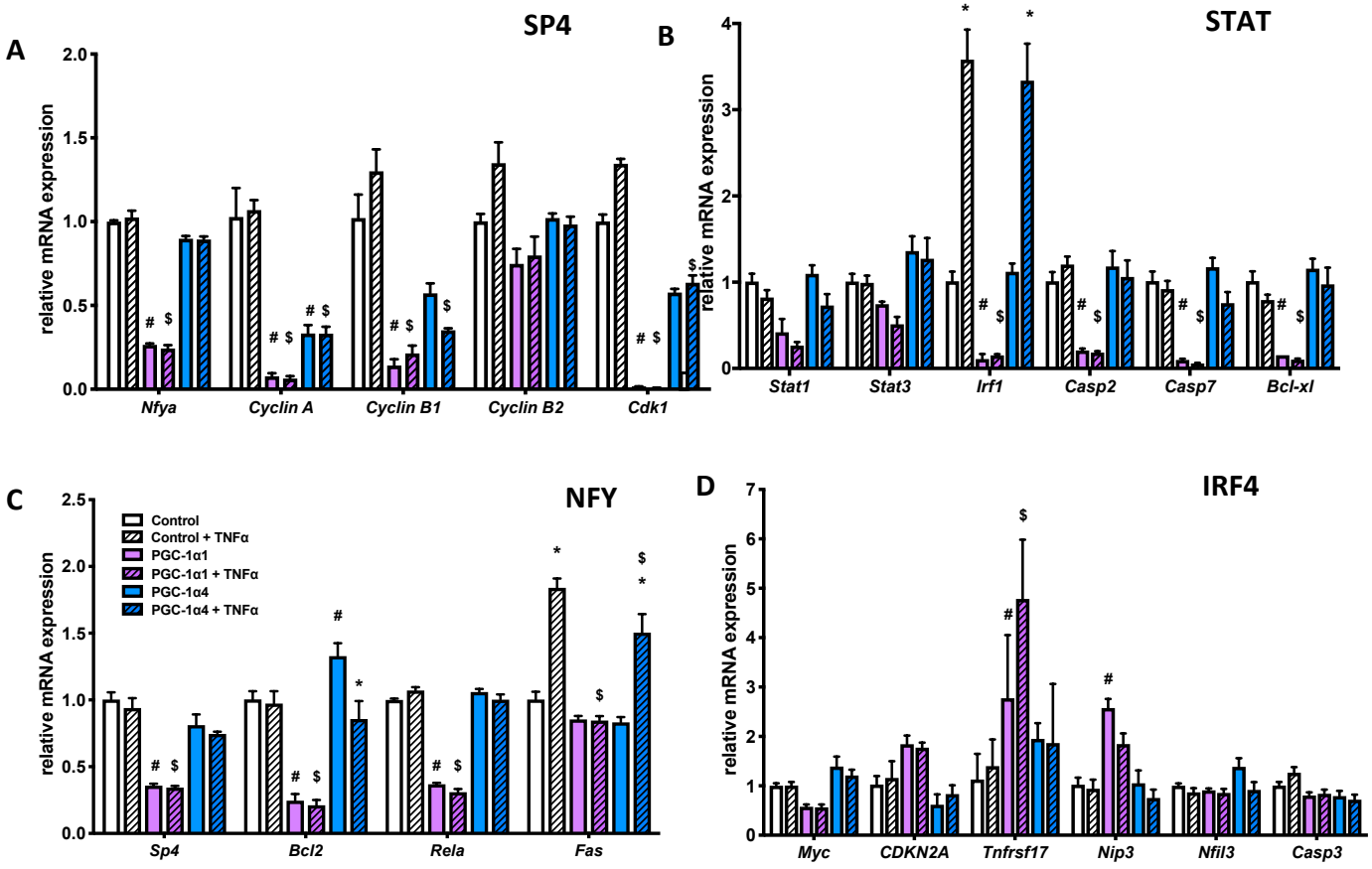

Supplementary Figure 5: Target genes downstream of transcription factors identified by iRegulon and DiRE. A-D) mRNA expression of primary mouse hepatocytes over-expressing PGC-1α1, PGC-1α4 or vector alone following 2-hr treatment with 2 ng/mL TNFα or vehicle (n=3). *p<0.05 effect of TNFα within each genotype. #p<0.05 Effect of PGC-1α1 or PGC-1α4 expression compared to Control. $p<0.05 TNFα response compared to Control + TNFα. Data are representative of at least 2 different experiments. Data represents biological replicates (n=3) from a representative experiment performed twice.

Supplementary Methods

Gene set enrichment analysis was performed using the javaGSEA software [PMID: 16199517] (version 3.0 – build: 01600) on chip data using the Gene Ontology processes [PMID: 30395331] gene set (number of permutations = 1000, Permutation type = gene_set, Chip platform = Affy_430_2.0_mgi (version 2011) from the Mouse Genome Database [PMID: 29092072]. The *Ppargc1a* probe (1434099_at) was removed prior to analysis to eliminate over-expression bias. GO processes displaying a FDR < 0.1 (more stringent than the usual FDR < 0.25 threshold [PMID: 16199517]) has been considered to be statistically significant.

Clustering based on PGC-1α4-regulated genes was performed using dChip software. Over-representation analysis (ORA) of Gene Ontology processes was performed with regulated genes displaying an adj. p-value < 0.01 and 2 fold changes (Log10 fold changes ≥ 0.3 or ≤ -0.3), by using ClusterProfiler [PMID: 22455463] and the mouse genome-wide annotation in R (www.r-project.org). The top 10 statistically over-represented GO processes (adj. p-value < 0.05, correction method = Bonferroni) were determined for each condition and represented as a dot plot. For 175 genes regulated oppositely by the variants, ORA of GO biological processes was performed using g:Profiler [PMID: 27098042] using the following parameters : adj. p-value < 0.05, correction method = g:SCS threshold.

Supplementary Table 1: Antibodies and Dilutions (Target, company, catalog number, dilution)

Target	**Company**	**Catalog Number**	**Dilution**
PGC-1α	Millipore	ST1202	1:500
V5	Thermo Scientific	MA5-15253	1:500
Hsp90	Cell Signaling	4874	1:2000
Cleaved Caspase 3 (Asp175)	Cell Signaling	9661	1:500
NFκB p50/p150	Abcam	ab32360	1:500
NFκB p65	Abcam	ab7970	1:500
IκBα	Abcam	ab32518	1:500
IKKβ	Abcam	ab32135	1:1000
Lamin B1	BioVision	3807	1:200
β-actin	Sigma	A5441	1:5000

Supplementary Table 2: Primers used for conventional PCR (listed in 5' – 3' direction)

Gene	Forward Primer	Reverse Primer	Band size
Mouse Primers			
PGC-1α1	GACATGTGCAGCCAAGACTC	CTCAAATGGGGAACCCTTGG	816
PGC-1α2 and *PGC-1α-b*	GATTGTCATCCATGGATTC	GTTCGCTCAATAGTCTTGTTC	325 / 826
PGC-1α3 and *PGC-1α-c*	CTCAGACCCACTATGCTGCTG	GTTCGCTCAATAGTCTTGTTC	302 / 818
PGC-1α4	GATTGTCATCCATGGATTC	CTGGAAGATATGGCACAT	812
NT-PGC-1α-a	GACATGTGCAGCCAAGACTC	CTGGAAGATATGGCACAT	822
NT-PGC-1α-c	CTCAGACCCACTATGCTGCTG	CTGGAAGATATGGCACAT	803

Genotyping primers			
Alb-Cre^{Tg}	Forward (Albumin promoter) TTAGAGGGGAACAGCTCCAGATGG	Reverse (Cre-recombinase) GTGAAACAGCATTGCTGTCACTT	
^{LSL}PGC-1α4	Forward (*Ppargc1a* exon 6) CCAAACCAACAACTTTATCTC	Reverse 1 (*Ppargc1a* intron 7) CCTTCTGATAAAGAGTCAACGC	Reverse 2 (*WPRE*) GGAGAAAATGAAAGCCATACGG
Ppargc1a$^{fl/fl}$	Forward (*Ppargc1a* intron 2) GGAGAGGTGTCAGGGAGAG	Reverse (*Ppargc1a* intron 2) CACAGCAGAGCACAAAGGA	
AltProm$^{fl/fl}$	Forward AGAGTCAGCAGAACAAGCGT	Reverse TGCTTTGCAGAGGTGCTCAT	

Supplementary Table 3: Primers used for quantitative real-time PCR (listed in 5' – 3' direction)

Gene	Forward Primer	Reverse Primer
Mouse Primers		
Birc2 (Ciap1)	TCTGCTGTGGCCTGATGTTGGATA	ATGGAGACTGCAGACTGGCTGAAA
Birc3 (Ciap2)	AACTCCCTTCGGGAAATTGACCCT	TTCTTTCCTCCT GGAGTTTCCGCA
Birc5 (survivin)	TGGACAGACAGAGAGCCAAGAACA	AGCTGCTCAATTGACTGACGGGTA
Ccl5 (Rantes)	GCTGCTTTGCCTACCTCTCC	TCGAGTGACAAACACGACTGC
IkBa (Nfkbia)	AGACATCCTTCCGCAAACTC	TAGGTCCTTCCTGCCCATAA
Il-10	GCTCTTACTGACTGGCATGAG	CGCAGCTCTAGGAGCATGTG
Mcp1 (Ccl2)	TCACCTGCTGCTACTCATTCACCA	TACAGCTTCTTTGGGACACCTGCT
Naip	AGATGAAGAGCTCACCACCTGCTT	AGTTCAGTCAGTCTCATGGCAGCA
Pgc-1α1/NT-PGC-1α-a	GGACATGTGCAGCCAAGACTCT	CACTTCAATCCACCCAGAAAGCT
Pgc-1α4/NT-PGC-1α-a,c	TCACACCAAACCCACAGAAA	CTGGAAGATATGGCACAT
Tnfα	CCCTCACACTCAGATCATCTTCT	GCTACGACGTGGGCTACAG
Tnfaip3 (A20)	AGCCAGAAGAAGCTCAACTGGTGT	TGCATGCATGAGGCAGTTTCCATC
Xiap	CCAGCCATGGCAGAATATGA	TCGCCTTCACCTAAAGCATAAA
Nfya	CTCTGTGCCTGCTATCCAAA	CCTCTTAAGGATGCGGTGATAC
Cyclin A	CACTGACACCTCTTGACTATCC	CGTTCACTGGCTTGTCTTCTA
Cyclin B1	GGTCGTGAAGTGACTGGAAA	GTCTCCTGAAGCAGCCTAAAT
Cyclin B2	CTCTGCAAGATCGAGGACATAG	TGCCTGAGGTACTGGTAGAT
Cdk1	CAGACTTGAAAGCGAGGAAGA	TCCTGCAGGCTGACTATATTTG
Cdc25c	TGCACAGTCAGAAGGAACTG	GGAGGAGAATTCACAGAGGAAC
Atad3a	GACAGGACAGCACAGTAGTAAG	AGCAGACCATCTCGTCAATG
Pim1	TTCAGGCAAACGGTCTCTTC	CCACGGATGGTTCTGGATTT
Csnk2a2	CACATAGACCTAGATCCACACTTC	CAAGGTGCCTGTTCTCACTAT
Btg2	CGCACTGACCGATCATTACAA	GGGTCCATCTTGTGGTTGATAC
Myc	CTC CGT ACA GCC CTA TTT CAT C	TGG GAA GCA GCT CGA ATT T
CDKN2A (p16)	CAT GTT GTT GAG GCT AGA GAG G	CAC CGT AGT TGA GCA GAA GAG
Tnfrsf17	GCCTGGAGTATACAGTGGAAGA	CGGGAAGAAATGGTCAGAATCC
Nip3	GACGAAGTAGCTCCAAGAGTTC	CCAAAGCTGTGGCTGTCTAT
Nfil3	GGTTTCCGAAGCTGAGAATTTG	AGATCGGTTGTGTGGCTATG
Casp3	AGTGGGACTGATGAGGAGAT	GTAACCAGGTGCTGTAGAGTAAG
Sp4	TTTCTCAGCCAGCTTCTAGTTC	GGGTGGAAGGATTACCTGATTT
Bcl2	GGAGGATTGTGGCCTTCTTT	GTTCAGGTACTCAGTCATCCAC
RelA (p65)	GAGAAGCACAGATACCACCAAG	GAGATTCGAACTGTTCCTGGTC
Fas	CCAAGTGCAAGTGCAAACCAGACT	AGGATGGTCAACAACCATAGGCGA
Human Primers		
HPRT	GGCCAGACTTTGTTGGATTTG	TGCGCTCATCTTAGGCTTTGT
Pgc-1α1/NT-PGC-1α-a	GGACATGTGCAACCAGGACT	CACTTGAGTCCACCCAGAAAGCT
Pgc-1α4/NT-PGC-1α-a,c	TCACACCAAACCCACAGA	CTGGAAGATATGGCACAT